Environmental Earth Sciences (2024) 83:264
https://doi.org/10.1007/s12665-024-11465-w

ORIGINAL ARTICLE

Isolated overburden grout injection technology mining and grouting parameters discussion and optimization

Ya-xing Li[1] · Jun Ma[2] · Ke-ming Yang[1] · Ke-gui Jiang[1] · Xin-ru Gu[1] · Li-shun Peng[1] · Xin-yang Chen[1]

Received: 13 November 2023 / Accepted: 29 January 2024 / Published online: 16 April 2024

Abstract
The Isolated Overburden Grout Injection Technology is employed for the "Three down" coal resource mining, ground subsidence management, and fly ash waste treatment, exemplifying the concept of environmentally friendly mining. The analysis of Isolated Overburden Grout Injection Technology can be effectively conducted utilizing the large-deflection inclined thin plate combined with the slurry model. However, differences in stratigraphic parameters, such as main roof and principal key strata (PKS), among different mines, as well as variations in design parameters like working face dimensions, mining height, coal seam angle of inclination, mining speed, and grouting parameters such as the number of grouting holes, start and finish times. These parameters lead to variations in outcomes such as *PKS* deflection and Bed-separation development, as well as the maximum subsidence and extent of the ground subsidence basin. To guarantee accurate and effective safeguarding of village structures, exploitation of coal resources, and appropriate management of fly ash waste, it is crucial to assess each parameter's influence in the model thoroughly. This analysis aims to clarify the mining and grouting process and enhance the logical design of the essential parameters. This paper classifies and examines the influence of each parameter on the results, utilizing the case study of the 7221 work face grouting operations in Huaibei, Anhui Province, China. The mining and grouting parameters were re-optimized to meet the protection requirements of the Gaochangying and Houlou Gaojia villages. The changes assessed the possible advantages of enhancing the initial design of coal seam resources and including fly ash backfill.

Keywords Key strata theory · Isolated Overburden Grout Injection Technology · Large deflection thin plate · Ground subsidence control · Parameters optimization

✉ Ke-ming Yang
ykm69@163.com

Ya-xing Li
yaxing_98@163.com

Jun Ma
1483361693@qq.com

Ke-gui Jiang
austjkg@163.com

Xin-ru Gu
319732572@qq.com

Li-shun Peng
2531511161@qq.com

Xin-yang Chen
cxy_sdkj@126.com

[1] College of Geoscience and Surveying Engineering, China University of Mining and Technology-Beijing, Beijing 100083, China

[2] General Defense Geological Survey Department, Huaibei Mining Co., Ltd., Huaibei 235000, China

Introduction

Following a prolonged time of mining operations in China, it has been noted that coal reserves are primarily concentrated in three specific sites known as the "Three Down" regions, which encompass structures, water bodies, and railroad (Yang and Zhang 2012; Wang, et al. 2022). Implementing sustainable mining techniques has led to the widespread adoption of filling mining technology to extract coal resources (Qian et al. 2003). By implementing cutting-edge mining technology, we can ensure the efficient extraction of coal resources and the seamless reintegration of gangue waste into the mine site. Implementing measures to reduce ground deformation and ensuring the proper disposal of waste material during mining operations can reduce environmental contamination and promote the adoption of environmentally friendly and sustainable coal mining practices (Jiang et al. 2019; Yin et al. 2020). The mining process can be categorized into two groups depending on waste recharge placement: extraction area filling mining (Zhu et al. 2011) and bed-separation filling mining. The extraction area filling mining mostly entails depositing waste materials into the allocated extraction area following the extraction of coal seams. The categorization of filling materials is determined by their physical state, encompassing water–sand filling (Bo et al. 2023), solid filling (Yin et al. 2020; Bo, et al. 2023), paste filling (Huang et al. 2011; Liu et al. 2012), and slurry filling (Li et al. 2020). Bed-separation filling mining involves the injection of filler material into a cavity, primarily using the Isolated Overburden Grout Injection Technology. Filling the extraction area has several advantages, such as streamlined operational operations, efficient handling of waste materials, and the use of existing technological breakthroughs. Implementing the Isolated Overburden Grout Injection Technology has been demonstrated to have a negligible effect on regular mining operations at work. This approach also enables enhanced control over ground subsidence, minimizing the risk of harm to adjacent structures (Wang et al. 2018; Zhu et al. 2017).

The deterioration of rock strata caused by excessive underground mining and the separation of layers is a complex phenomenon that is impacted by several geographical and temporal factors (Tan et al. 2015; Li et al. 2015). The Bed-separation is developed based on the key stratum idea proposed by the Chinese scholar Qian Minggao (Li et al. 2018; Ju and Xu 2013). The stratification of rock layers with varying degrees of hardness and softness led to strata formation. One particular form of stratum that stands out is the key strata, known for its strong and rigid composition and impressive ability to withstand bending and stretching forces. These essential layers play a vital function in preserving the bending of all the rock layers. More precisely, the thicker rock layer, which has a high Young's modulus and tensile strength, deflects less than the underlying rock layer. This disparity results in the creation of gaps between the two layers, which are referred to as bed-separation cavities.

The Isolated Overburden Grout Injection Technology entails the construction of boreholes in the ground and injecting a high-pressure slurry into voids created during the displacement of rock formations. This method harnesses the stress exerted by the slurry to provide support for the crucial layers above (Li et al. 2023). Initially, Soviet scientists implemented grouting as a method to alleviate subsidence. Tests examining this technique were subsequently carried out in Poland during the 1980s (Palarski 1989). The implementation of this technology in Australia began in 2000 (Zhao et al. 2004; Alehossein 2009). Chinese researcher Fan Xueli conducted a pioneering engineering experiment on the Isolated Overburden Grout Injection Technology 1985 at the Tiger Terrace Mine in Fushun (Xu et al. 2015). However, the current rate at which subsidence is being reduced is not very high, leading to a large amount of ground sinking that does not adequately protect above-ground structures. In 2000, Xu Jialin implemented the "Isolated Overburden Grout Injection" technique to guarantee that ground surface deformation stays within the prescribed threshold, as mandated by the building protection standard (Xuan and Xu 2017). As mentioned earlier, the technique was employed at the Huaibei mining region in Anhui Province, China. The implementation of this technique led to the reduction of ground deformation during mining operations. The goal of coal mining without the necessity of relocating villages was accomplished (Xuan et al. 2020, 2015).

Scholars mostly utilized a technique in which they evaluated the spatial volume change by subtracting the volume of the extraction area from the volume of the injected slurry, following the introduction of the Isolated Overburden Grout Injection technology proposal. Afterward, the researchers utilized the Probability Integration Method (PIM) in their investigation to calculate the extent of ground subsidence (Xuan and Xu 2017; Xuan et al. 2016). The existing model cannot sufficiently account for the intricate interaction of coal seam mining, injection activities, and the geological layers. The author of this study introduces a theoretical framework for analyzing large-deflection inclined thin plates. It investigates the deflection process, the dynamic development of bed-separation, and the ground deformation of the key strata beneath the mining activities. Then, the mixture was inserted into the slanted Bed-separation chambers, where the concepts of non-Newtonian fluid dynamics and slurry rheology were used to study the effects of stress reduction on the important layers. In addition, a model was created to examine the behavior of inclined thin plates with significant deflection when exposed to the effects of the slurry. The model was efficiently employed in the 7221 work face of a mine in Anhui, China. This application showcased the mechanical interaction between coal seam mining, grouting activities, and the ground.

After formulating and implementing the model for a large-deflection inclined thin plate affected by slurry in practical mining operations at different work faces in various mines, it is necessary to resolve a set of variables inside the model. The variables being examined pertain to three key areas: the physical attributes of the overlying layers, the configuration of the mining operation at the active area, and the factors associated with the slurry design. The overarching strata primarily include physical factors, such as the spatial organization of the main layers, their thickness, and the lithologic properties of the layers. The key parameters taken into account in work face design include the dimensions of the mining area, including length, width, and height, along with the level of slope of the coal seam. In addition, factors such as mining velocity are also considered. The slurry design parameters include multiple aspects, such as the number of holes, start and end time, and other relevant physical parameters. The physical parameters of the Isolated Overburden Grout Injection technology significantly impact its design and the subsequent *PKS* deflection and ground sinking. Therefore, this study utilizes a previously developed model of a thin plate inclined at a considerable angle, affected by slurry. The purpose is to categorize and analyze how stratigraphic characteristics, work face and slurry design parameters affect the *PKS* and ground subsidence deflection. In addition, a thorough collection of parameters was obtained during a mining operation at the 7221 work site in Anhui Province, China. These criteria include logical assumptions and have helped improve the efficiency of the mining and grouting procedures at the indicated work site. More evaluation is necessary to evaluate the model's universality and stability, improve its adaptability to various mining regions, and provide a stronger theoretical basis and practical recommendations for the Isolated Overburden Grout Injection technology.

The study area and the engineering geology

General overview of the study area

This study selected 7221 work face of a mine in Huaibei, Anhui Province, China, with mining start and end time from December 6, 2017, to June 3, 2018. The 7221 work face has a strike length of 588 m, an inclination length of 100 m, a striking dip of 6.8°, an inclination dip of 8.2°, and a mining thickness of 4.6 m. The corner point of the cutting line of the working face and the upper mountain boundary is – 351 m, the corner point of the closing line and the lower mountain boundary line is – 433.4 m, and the ground elevation is 28 m. The thickness of the bedrock is 220.58 m, and the thickness of the thick loose layer ranges from 158.42 m to 240.82 m. The spatial distribution and geological structure of the working face are shown in Fig. 1. Due to the inclination angle of the coal seam, the bedrock above the opening and closing line is loaded by a loose layer with a thickness difference of 82.4 m after mining the coal seam with a longer mining length.

Grouting operations commenced on January 8, 2018, within the designated grouting hole identified as No. 1. Prior to that, the mining operation had excavated a distance of 142 m in the 7221 work face. The daily mining distance of the 7221 work face was recorded starting from the date of grouting hole No. 1. The recorded data is presented in Fig. 2. The mining operations persisted for 150 days, concluding on June 3, 2018. The mining process of the work face remains unaffected during the implementation of Bed-separation grouting, allowing for continuous excavation at a consistent pace.

The engineering geology

Analyze the rock distribution and physical properties of rock strata in a drill hole data above the working face, and determine the distribution of key strata of bedrock above the working face. The information of each rock strata number, name, thickness, depth from the surface, rock strata classification schematic, and key strata distribution were obtained from drilling, as shown in Fig. 3.

Concerning the physical properties of each rock strata in the actual borehole measured by the mine and related studies, the parameters of each rock stratum in the above borehole, such as density, tensile modulus, shear modulus, elastic modulus, cohesion, internal friction angle, and Poisson's ratio, were obtained as shown in Table 1.

Grouting parameters for 7221 work face

The 7221 work face mining method incorporates the utilization of Bed-separation grouting as a technique to manage waste material and mitigate ground subsidence. Five grouting holes were strategically positioned to facilitate the grouting process within the internal cavity of the Bed-separation layer above the 7221 work face. Table 2 displays the quantity of grouting holes, spatial coordinates, drilling depth, and the initiation and cessation time of grouting within the grouting holes.

In examining the daily grouting volume and grouting hole pressure of each grouting hole, specifically from No. 1 to 5, after the initiation of grouting in grouting hole No. 1, the findings are depicted in Fig. 4. As of July 14, 2018, the grouting operations were successfully concluded in grouting holes No. 4 and No. 5, totaling 187 days. The daily total grouting volume, denoted by the red line, refers to the cumulative quantity of grouting material injected into each grouting hole within a given day. When the distance of mining is limited, the resulting volume of the cavity formed during Bed-separation is reduced. The injected grout volume is rather minimal, thus obviating the necessity for pressure augmentation. The slurry effortlessly permeates the Bed-separation cavities. Subsequently, following the expedited extraction of the 7221 work face, a simultaneous grouting process was employed to fill several grouting holes. The daily grouting volume can exceed 800,000 kg, with a consistently steady grouting pressure.

In conclusion, as the mining activity draws to a close, it is noteworthy that the Bed-separation cavity has been successfully filled with slurry. However, injecting the slurry at an elevated pressure is imperative to ensure optimal results. Additionally, it is worth mentioning that the daily amount of slurry injection has decreased.

Fig. 1 Schematic of 7221 work face and grout holes parameters

Stratigraphic parameter effects on *PKS* deflection and Bed-separation development

As the inclined working face descended, the rock strata within the caved zone experienced breakage and yielded. With the working face inclined downward for mining, the regional division of the collapsed, fractured, and continuous bending zones above the mining zone and the development of Bed-separation under the principal key strata in the bending zone are shown in Fig. 5. Additionally, it depicts the development of the deviated strata beneath the primary key strata inside the constrained zone. The mudstone immediately above the coal seam is called the second mudstone, while the major roof above the coal seam is composed of the third siltstone. The soft rock separation between the fourth and tenth seams is located within the area affected by cave-ins. The 11th layer of fine sandstone plays a crucial role inside the second geological layer. In contrast, a portion of the less-consolidated rock from the 12th layer is within the fractured zone. Regarding the breakage distance and the angle between the fracture trace in the table, the predicted height of the caved zone resulting from the mining of work face 7221 is 22.93 m, whereas the fractured zone's height is 21.05 m.

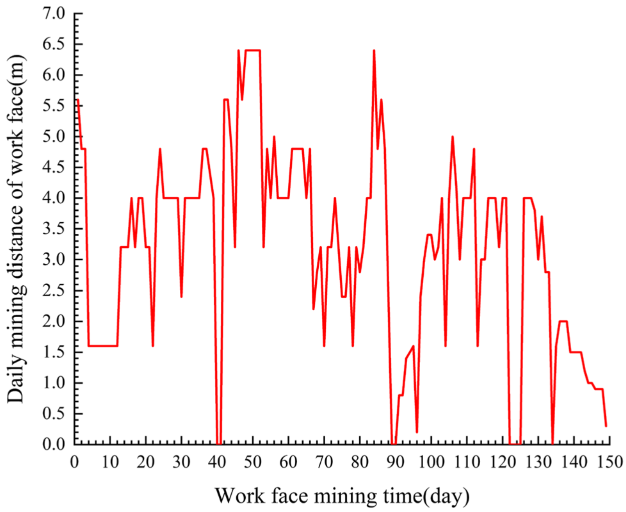

Fig. 2 Daily mining distance statistics for 7221 work face

The strata that remain in proximity to the ground are situated within a delimited area, encompassing a 14th layer composed of siltstone, which serves as the third significant stratum, a 19th layer consisting of fine sandstone, referred to as the *PKS*, and a 41st layer characterized by a substantial accumulation of loose strata. In this particular instance, it has been observed that the siltstone comprising the primary stratum inside the collapsed region has had a downward displacement. The fine sandstone constituting the secondary stratum within the restricted zone has experienced fracturing. Furthermore, the region of the Bed-separation has undergone compression, resulting in compaction. The siltstone found in the third key strata and the fine sandstone observed in the 19th *PKS*, both located inside the flexural zone, exhibit the presence of Bed-separation cavities. Notably, the Bed-separation cavities below the *PKS* demonstrate a greater height and larger volume.

Each rock stratum above the 7221 work face consists mostly of two critical strata that will directly influence the process of coal seam excavation and slurry filling mining. Upon excavation of the 7221 work face, it is anticipated that the initial uppermost strata, known as the main roof, will experience fracturing and subsequent collapse. The fracture trace angle of the main roof thin plate and the initial and periodic pressure steps are directly influenced by the physical parameters of the main roof strata. The grouting slurry is situated within the Bed-separation cavity beneath the *PKS*. The physical characteristics of the *PKS* directly influence the progression of Separation and, therefore, affect the parameter design of the Bed-separation grouting. This section focuses on the selection of thicknesses and physical qualities of the *PKS* in the primary roof and curvature zone located above the coal seam. The objective is to investigate the impact of stratigraphic parameters on the *PKS* deflection and Separation.

Influence of main roof thickness and lithologic parameters on the top plate

The initial stratum within the cave zone, known as the key strata, experienced breaking, resulting in increased strain on the roof above the active mining area. The main roof thin plate's fracture trace angle and breakage distance are determined using the large-deflection inclined thin plate model. These calculations are a theoretical foundation for predicting the initial and periodic incoming pressure steps. In general, an increase in the thickness of the main roof is associated with a decrease in the angle between the initial fracture trace and the working face. Simultaneously, there is an increase in the magnitude of the initial incoming pressure step. However, it is important to note that this increase in incoming pressure results in a more pronounced impact.

The actual detection of the major roof above the 7221 work face is siltstone with a thickness of 13.15 m. The fracture trace angle and incoming pressure stepover data acquired by computation are presented in the initial row of Table 3. This study assumes a thickness of 8.15 m and 18.15 m for the main roof. The rock layers are replaced from siltstone to fine sandstone for computation. The corresponding results can be found in the remaining rows of Table 3. The practical computations of the model of a thin plate with large deflection and inclination exhibit similarities to the corresponding theoretical framework. Specifically, when the primary roofs are thicker, the fracture trace angle decreases, while the first incoming pressure step increases.

Effect of *PKS* thickness and lithologic parameters on *PKS* deflection and Bed-separation development

The primary location for the grouting process, Isolated Overburden Grout Injection, is the Bed-separation cavity under the *PKS* within the collapsed zone. Hence, the physical characteristics of the *PKS* influence the bending of slender plates and hold significance in forming Separation. The *PKS* was acquired as a finely grained sandstone with a thickness of 18 m, as determined by the drilling parameters. The first row of Table 4 presents the outcomes of the large-deflection inclined thin plate model, which was utilized to compute the maximum deflection height of the *PKS* and the development of bed-separation. Subsequently, this study posits three different thicknesses for the *PKS* layer, namely, 8 m, 13 m, and 21 m. The *PKS* rock layer is then substituted with siltstone, and calculations are performed to determine the initiation and termination positions of *PKS* deflection, the magnitude of *PKS* deflection, the volume of the resultant void space, and the maximum height of Bed-separation development. The findings are presented in further rows of Table 4. As the thickness of the *PKS* decreases, the deflection value of the 7221 work face increases, accompanied by an increase in the amount of

No.	Thickness(m)	Depth(m)	Lithology	Key Strata	Legend
41	202.01	202.01	Loose layer		
40	1.7	203.71	Mudstone		
39	4.1	207.81	Mudstone		
38	4.9	212.71	Coarse sandstone		
37	8.0	220.71	Fine sandstone		
36	5.75	226.46	Mudstone		
35	15.2	241.66	Coarse sandstone		
34	4.35	246.01	Mudstone		
33	11.2	257.21	Coarse sandstone		
32	3.85	261.06	Coarse sandstone		
31	5.25	266.31	Mudstone		
30	1.5	267.81	Mudstone		
29	6.9	274.71	Coarse sandstone		
28	3.65	278.36	Coarse sandstone		
27	3.2	281.56	Mudstone		
26	4.8	286.36	Siltstone		
25	6.75	293.11	Mudstone		
24	3.4	296.51	Siltstone		
23	15.95	312.46	Mudstone		
22	3.2	315.66	Siltstone		
21	5.1	320.76	Mudstone		
20	4.6	325.36	Mudstone		
19	18.0	343.36	Fine sandstone	PKS	
18	4.6	347.96	Siltstone		
17	6.0	353.96	Mudstone		
16	5.2	359.16	Siltstone		
15	3.35	362.51	Mudstone		
14	8.65	371.16	Siltstone	KS 3	
13	2.45	373.61	Fine sandstone		
12	20.05	393.66	Mudstone		
11	6.0	399.66	Fine sandstone	KS 2	
10	1.55	401.21	Mudstone		
9	0.4	401.61	Coal		
8	0.95	402.56	Mudstone		
7	1.65	404.21	Mudstone		
6	0.35	404.56	Coal		
5	2.15	406.71	Mudstone		
4	1.1	407.81	Fine sandstone		
3	13.15	420.96	Siltstone	KS 1	
2	1.63	422.59	Mudstone		
1	3.78	426.37	Coal		

Fig. 3 Histogram of stratigraphic drill holes in the 7221 work face

Table 1 Reference table of physical properties of each rock strata in drill holes

Lithology	Density (kg/m^3)	Tensile strength (MPa)	Elastic modulus (GPa)	Shear modulus (GPa)	Cohesion (MPa)	Angle of internal friction (°)	Poisson's ratio
Loose layer	2200	0.1	0.3	0.115	1.5	20	0.3
Mudstone	2600	1.2	13	5.28	1.73	31.3	0.23
Siltstone	2700	4.41	22.9	9.7	4.74	31.4	0.18
Coarse sandstone	2700	4.02	34.2	14.37	5.17	37.5	0.19
Fine sandstone	2700	4.34	34.1	14.96	3.15	35.9	0.14
Coal	1300	0.3	5.6	2.15	0.5	25	0.3

Table 2 Parameters of grouting holes of 7221 work face

Grouting holes number	Grouting holes x-axis coordinates (m)	Grouting holes y-axis coordinates (m)	Grouting holes depth (m)	Grouting start time	Grouting finish time
No.1 grouting hole	3,709,975	451,047	– 295.7	January 8, 2018	March 12, 2018
No.2 grouting hole	3,710,032	451,055	– 303.4	January 29, 2018	July 14, 2018
No.3 grouting hole	3,710,183	451,064	– 325.2	March 3, 2018	May 22, 2018
No.4 grouting hole	3,710,232	451,072	– 331.2	March 17, 2018	July 14, 2018
No.5 grouting hole	3,710,305	451,079	– 329.2	April 17, 2018	July 14, 2018

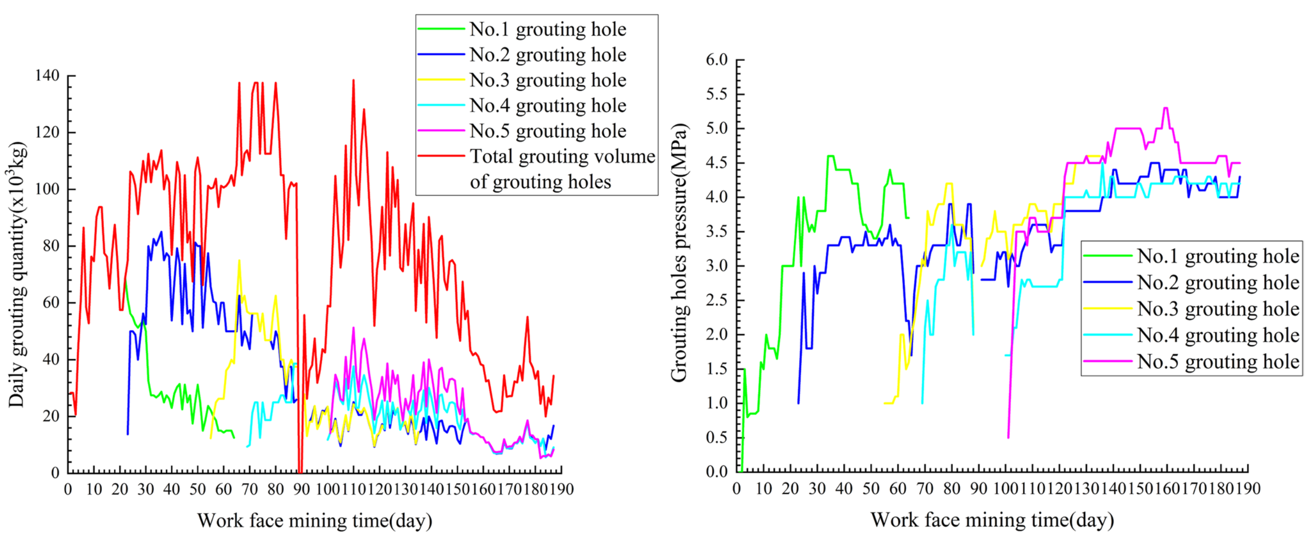

Fig. 4 Grouting volume and grouting stress statistics for grouting holes No. 1–5

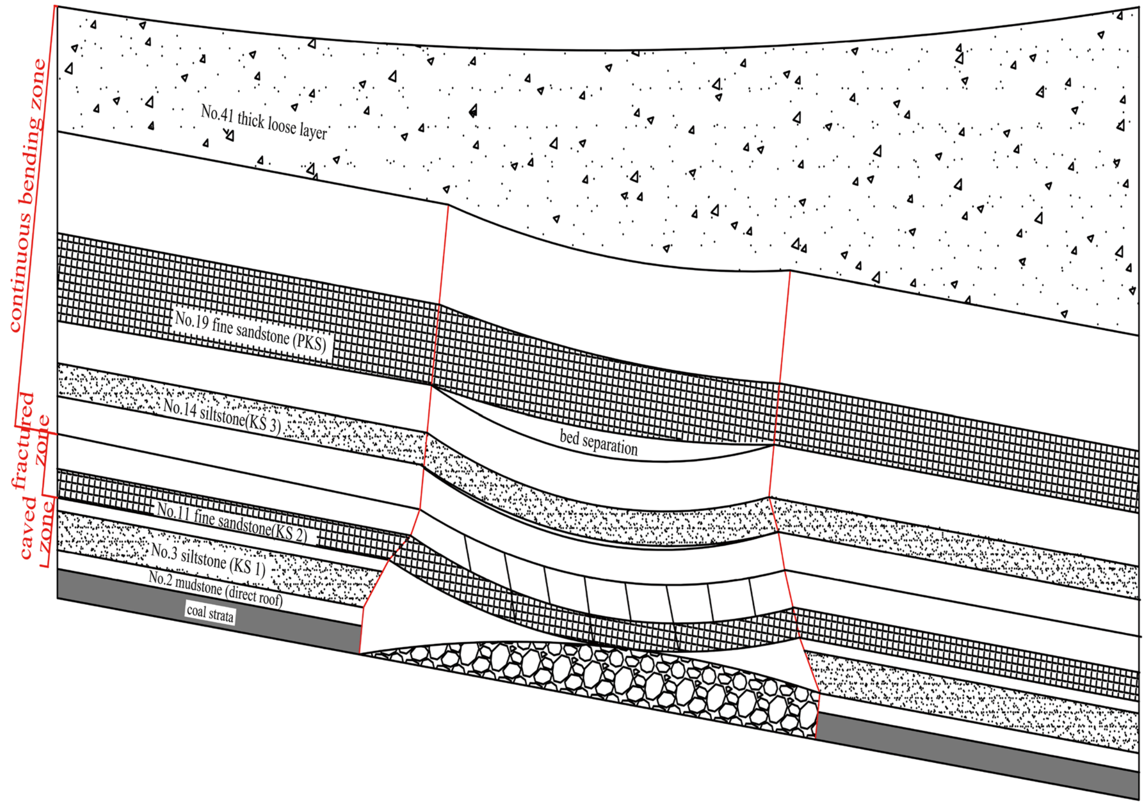

Fig. 5 Bending and breaking of key strata caused by mining, regional division of "vertical three zones", dynamic development of Bed-Separation

Table 3 Results of the effect of different parameters of the main roof on the fracture trace and the step of incoming pressure

Main roof thickness and lithotype	Initial breakage distance (m)	Initial fracture trace angle (°)	Periodic breakage distance (m)	Periodic fracture trace angle (°)
13.15m siltstone	36	57.2	17	54.3
8.15m siltstone	25	60.7	16	54.8
18.15m siltstone	46	55.4	17	54.3
13.15m fine sandstone	36	57.1	17	54.3

Table 4 Effect of different parameters of *PKS* on the development of *PKS* deflection and Bed-separation

PKS thickness and lithotype	*PKS* deflection start position (m)	*PKS* deflection end position (m)	*PKS* maximum deflection value (mm)	*PKS* deflection space volume (m^3)	Maximum height of Bed-separation (mm)
18m fine sandstone	29	549	1868	25,638	1725.2
13m fine sandstone	29	549	2068	30,400	1525.2
8m fine sandstone	29	549	2885.6	36,721	707.6
21m fine sandstone	29	549	1638	20,456	1955.2
18m siltstone	31	548	1691.6	27,954	1900.4

space resulting from the deflection. Simultaneously, due to the heightened *PKS* deflection value, the vertical expansion of the Bed-separation development is constricted, reducing the volume of the Bed-separation cavity and the injected slurry. The reduced thickness of *PKS* results in a decrease in waste disposal volume and an increase in the complexity of ground subsidence control. When building an Isolated Overburden Grout Injection face, it is important to consider the thickness of the *PKS*.

Effect of work face design parameters on *PKS* deflection, Bed-separation development, and ground subsidence

The initial step involves acquiring the drilling data and afterward analyzing the depth of the coal seam, as well as identifying the composition and thickness of each rock stratum above it. Following this assessment, the subsequent phase entails formulating the coal seam mining design parameters. The primary factors considered in work face design are the dimensions of the mining area, including length, width, and height, as well as the degree of inclination of the coal seam. The design parameters of the work face have a dual impact on the subsidence basin and the development of the Separation below the *PKS*. First, they cause the *PKS* to deflect, affecting the expansion of the subsidence basin at the ground level. Second, these parameters also influence the design considerations for subsequent grouting of the Bed-separation slurry filling mining. Hence, in implementing Isolated Overburden Grout Injection Technology, it becomes imperative to develop a rigorous and precise mechanical model, appropriately determine the mining parameters of the work face, and ensure compatibility with the parameter design of the slurry filling.

Design length of 7221 work face

Given the hypothetical presence of an infinitely long coal seam, it is observed that the current mining length of work face 7221 is 588 m. However, for this discussion, it is now postulated that the mining length of work face 7221 is 3000 m. This study aims to conduct a graphical analysis of various parameters related to unpressurized grouting in mining operations. Specifically, we will examine the change in *PKS* deflection value, the volume of deflection space, the maximum subsidence value of the ground subsidence basin, the maximum height of the Bed-separation development, the volume of the Bed-separation cavity, and the injection ratio. These analyses will be conducted on the length of mining after extending the 7221 mining length.

7221 work face length effects on *PKS* deflection and ground subsidence

Upon assuming that the mining length of the 7221 work face is 3000 m, graphical representations were constructed to determine the *PKS* deflection value and the volume of deflection space. The outcomes of these calculations are presented in Fig. 6. The *PKS* deflection value gradually increases as the mining of 7221 work face progresses. This trend continues until a mining distance of 1455 m is reached; at this point, the *PKS* deflection value reaches its maximum value of 2214.8 mm. Subsequently, the *PKS* deflection value decreases as the mining distance increases. Specifically, when the mining distance reaches 3000 m, the *PKS* deflection value decreases to 2031 mm. As the mining progress advances in the 7221 work face, the volume of the *PKS* flexure space undergoes a corresponding increase. Upon reaching a mining distance of 3000 m, the flexure space attains its maximum volume, measuring 145712m^3.

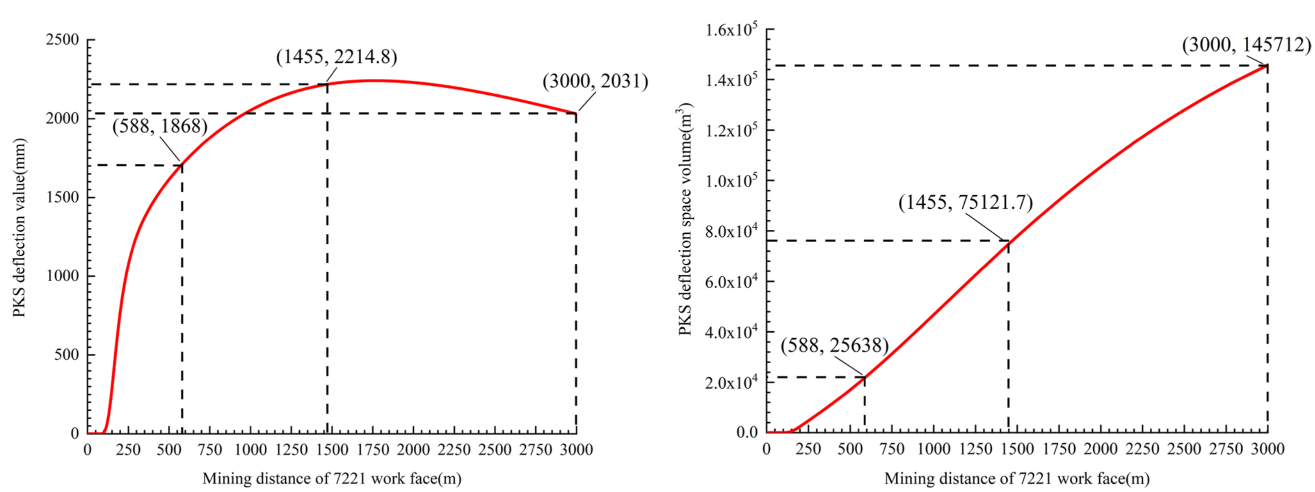

Fig. 6 *PKS* deflection value and volume of deflection space for hypothetical mining of 3,000 m of 7221 work face

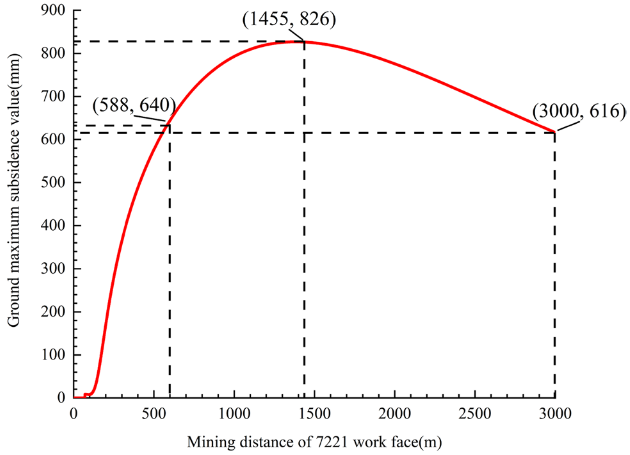

Fig. 7 Maximum subsidence value of ground subsidence basin assuming 3000 m mining of 7221 work face

Once the *PKS* flexure space volume is determined, the ground subsidence basin's inscribed function is formed based on equal volume. The calculation of the maximum subsidence value of the basin has been performed, and the outcomes are presented in Fig. 7. The mining width of 100 m for the 7221 work face is determined based on the strong flexural strength of the rock formation and the thickness of *PKS*, which is 18 m and has a high Young's modulus. However, this mining width is considered insufficient and may result in the maximum sinking value of the ground hole. When the mining distance of the 7221 work face reaches 1455 m, the deflection value of the *PKS* achieves its maximum value of 2214.8 mm. However, the maximum sinking value of the earth is only 826 mm. In the interim, it has been observed that the forward mining of the 7221 work face has resulted in the expansion of the ground subsidence basin. Consequently, the volume of the deflection space for the *PKS* has been progressively increasing. Furthermore, it

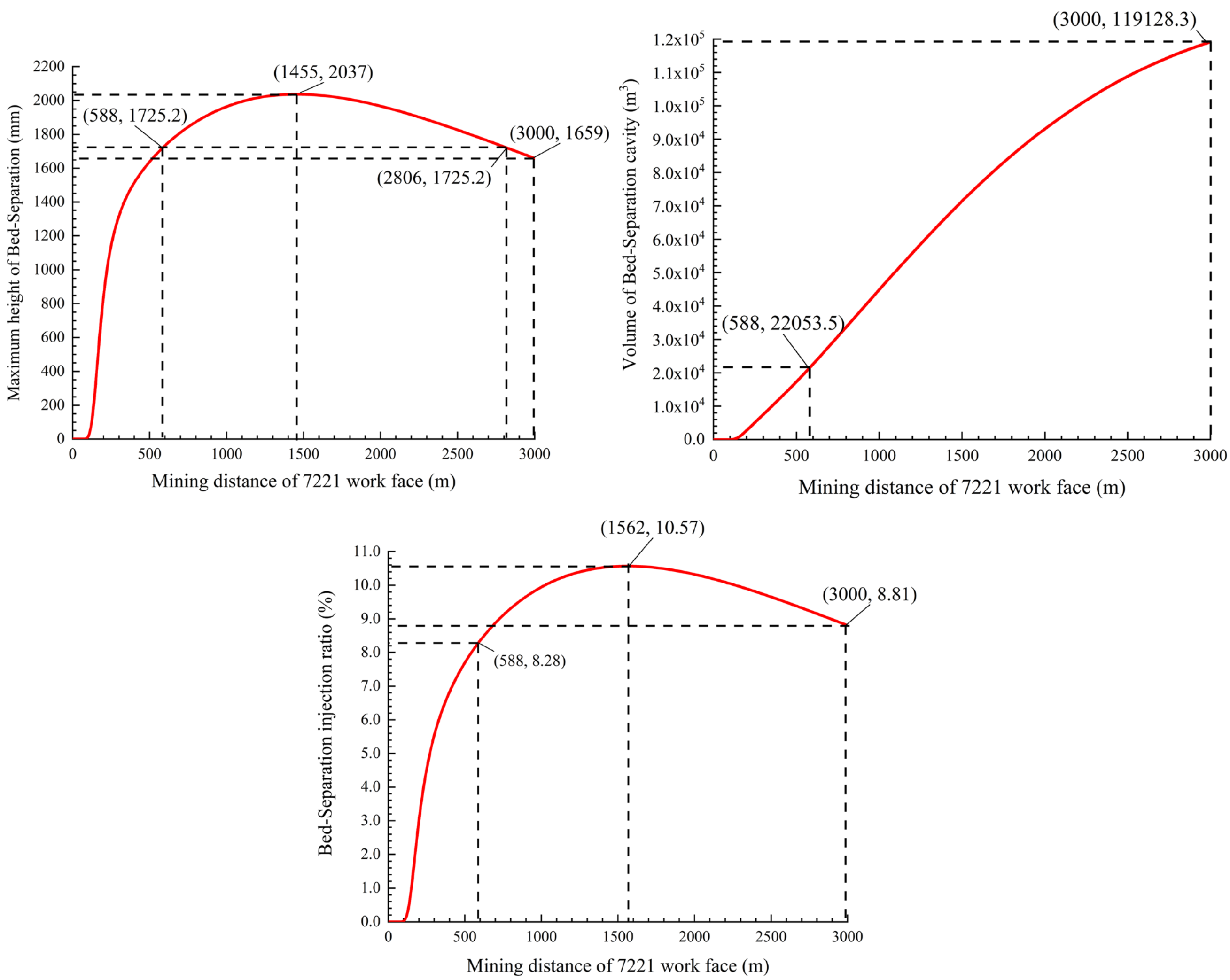

Fig. 8 Maximum height of Bed-separation development, Bed-separation volume, and non-pressurized Bed-separation grouting injection ratio for hypothetical mining of 3,000 m of 7221 work face

has been noted that once the maximum subsidence value is attained, the ground's subsidence value does not exhibit a decreasing trend as expected.

7221 work face length impact on grouting design

Given a mining length of 7221 work face, we can determine the maximum height of the Bed-separation development, the volume of the Bed-separation cavity, and the grouting injection ratio under no pressure. These results are depicted in Fig. 8. The grouting under pressure injection ratio is hypothesized to apply minimal pressure to the grouting hole, facilitating the smooth flow of slurry into the Bed-separation cavity. The grouting volume is determined by dividing the result by the volume of the extraction zone, yielding a percentage. As the mining operation progresses in the 7221 work face, the height of the Bed-separation development gradually grows. It reaches its peak value of 2037 mm when the mining distance reaches 1455 m. Subsequently, as the mining of the 7221 work face progresses, the *PKS* undergoes deformation, and the Separation gradually diminishes. The maximum height of the Bed-separation development reaches 1659 mm at a mining distance of 3000 m, smaller than the Bed-separation observed when the work face was mined at 588 m. The magnitude of the Separation is comparatively reduced to the dimensions seen during the mining of the work face. The highest vertical distance between two points is measured to be 1659 mm, significantly smaller than the distance of 588 m seen during the mining of the work face. As the mining process progresses in the 7221 work face, the cavity volume in the Separation area experiences a continuous increase. The volume of the cavity does not exhibit an increase and is better suited for the mining method involving the filling of bed-separation slurry. Hence, including the grouting injection ratio parameter in the absence of pressure demonstrates that as the mining face progresses, the actual injection ratio exhibits a pattern of initial increase followed by a subsequent decrease. This finding supports the argument that infinitely extending the advancing distance of the working face is inappropriate for Bed-separation grouting and mining.

Design width of 7221 work face

The design width of the work face is a critical factor in the Isolated Overburden Grout Injection design. It is necessary for the design width to adequately accommodate the mining process to ensure the formation of the Bed-separation cavity. The designated width of the 7221 work face is 100 m, indicating that it falls under the category of non-sufficient mining. Various assumptions have been made regarding mining widths, including 60 m, 140 m, 180 m, and 220 m. These assumptions regarding the width of the work face contribute to the transition of the Bed-separation 7221 work face from non-sufficient mining to sufficient mining. The purpose of this study is to visually analyze the relationship between the width of the work face design and several factors, including *PKS* deflection, deflection space volume, maximum ground subsidence value, height of Bed-separation development, and Bed-separation cavity volume. The objective is to see how these factors change as the seam width increases.

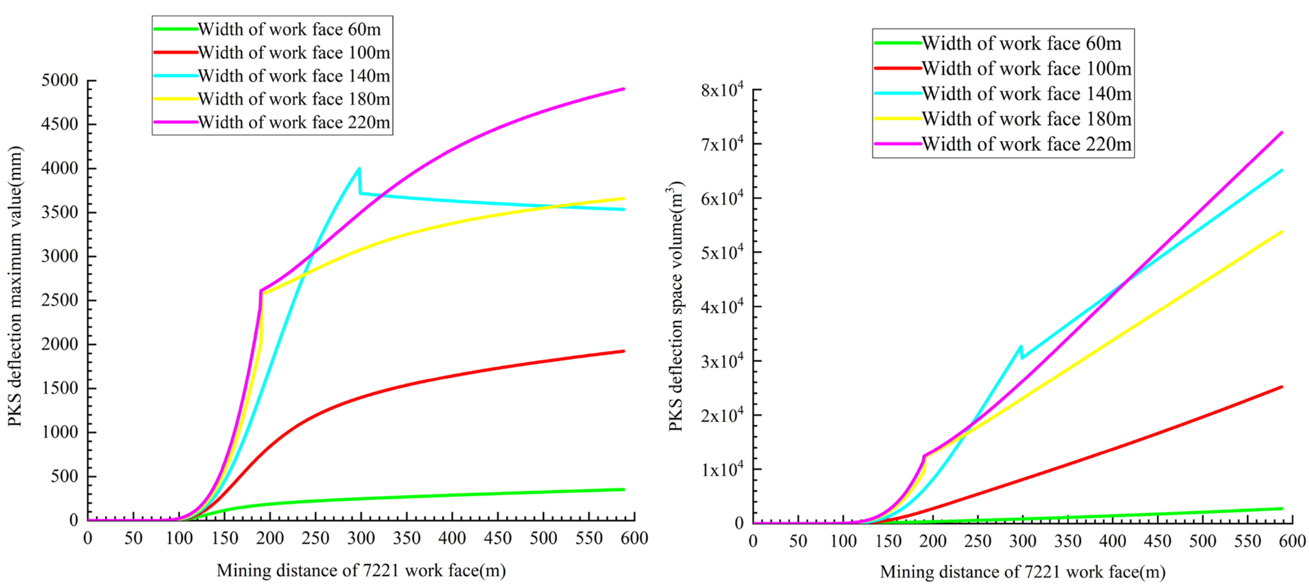

Fig. 9 *PKS* deflection values and deflection space volume for different mining widths assuming 7221 work face

7221Work face width effects on *PKS* deflection and ground subsidence

Given the hypothetical scenario of an infinitely expandable coal seam in terms of strike and inclination, it is permissible to consider that the 7221 work face has been designed with varying mining widths. Figure 9 presents *PKS* deflection and deflection space volume outcomes for mining widths of 60 m, 100 m, 140 m, 180 m, and 220 m. The deflection value of *PKS* exhibits a quick increase with the expansion of mining breadth, assuming adequate mining conditions while maintaining a constant distance. At a mining distance exceeding 200 m, the *PKS* deflection value and the volume of the deflection space are seen to be more than double compared to a mining width of 100 m. The work face design in question (7221) has a propensity toward adequate mining. It has been observed that the rate of growth in the deflection value of the *PKS* and its maximum value are not significantly influenced by an increase in width. Nevertheless, both factors exhibit a significant magnitude, which poses a disadvantageous situation for employing mining techniques to mitigate ground sinking.

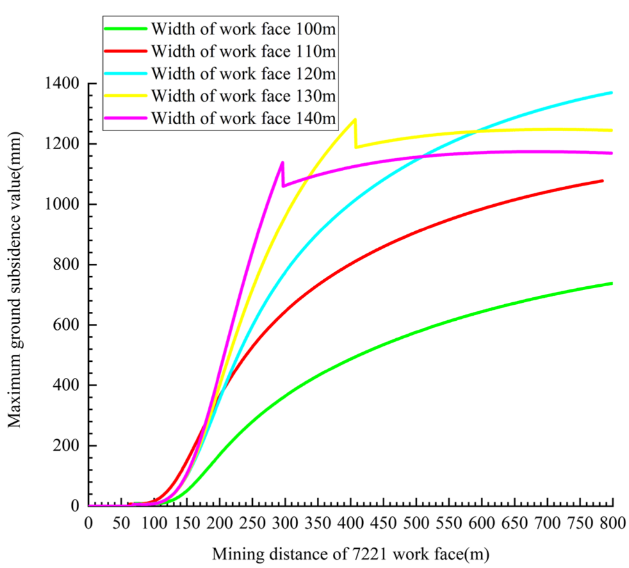

Fig. 10 Maximum subsidence values of the ground assuming different mining widths for 7221 work face

The *PKS* flexure space volume with 7221 work face mining is analyzed in this study. The analysis considers various mining widths and thicknesses, assuming an increase in these parameters. The concept of equal volume is employed to calculate the inscribed function of the ground subsidence basin. Additionally, the maximum value of ground subsidence is determined. The results are presented in Fig. 10. Due to different mining widths, the ground subsidence exhibits significant variation in the absence of Bed-separation slurry filling mining. When the mining width is 60 m, the ground surface experiences a maximum subsidence value of around 100 mm. When the mining width is 100 m, the ground experiences a maximum subsidence value of 640 mm. When the mining breadth of the working face reaches 140 m, it can be said to have reached the stage of sufficient mining. There is a substantial alteration in the regulation governing the fluctuation of subsidence values. The subsidence value reaches a maximum of over 1400 mm. Subsequently, as the mining breadth of the working face expands to 180 m and 220 m, the subsidence pattern of the ground surface reemerges. The subsidence value is twice the mining width of 100 m. Subsequently, as the working face width expanded to 180 m and 220 m, the ground subsidence pattern reoccurred, doubling the subsidence magnitude compared to the mining width of 100 m.

Table 5 presents the statistical outcomes of basin expansion length, width, maximum ground subsidence value, basin volume, and coordinates of the center point of the subsidence basin in the ground subsidence basin after the design of various mining widths. Based on the statistical findings, it is evident that, while disregarding the slurry parameter design for Isolated Overburden Grout Injection, opting for Longwall mining and designing a mining width of 180 m is a more favorable alternative for mining the 7221 work face.

7221 Work face width impact on grouting design

The parameters, including the height of Bed-separation development, the volume of the Bed-separation cavity, and

Table 5 Deformation results of ground subsidence basin with different mining widths for assuming 7221 work face

Design width of work face (m)	Length of subsidence basin (m)	Width of subsidence basin (m)	Ground maximum subsidence value (mm)	volume of subsidence basin (m^3)	Coordinates of center point of ground subsidence basin
Width of work face 60m	791	333	82	3272	(308.7,56)
Width of work face 100m	795	376	640	30,300	(310.5,78)
Width of work face 140m	799	420	1457	76,935	(312.6,100)
Width of work face 180m	803	464	1079	63,575	(314.7,122)
Width of work face 220m	807	518	1308	85,194	(316.3,144)

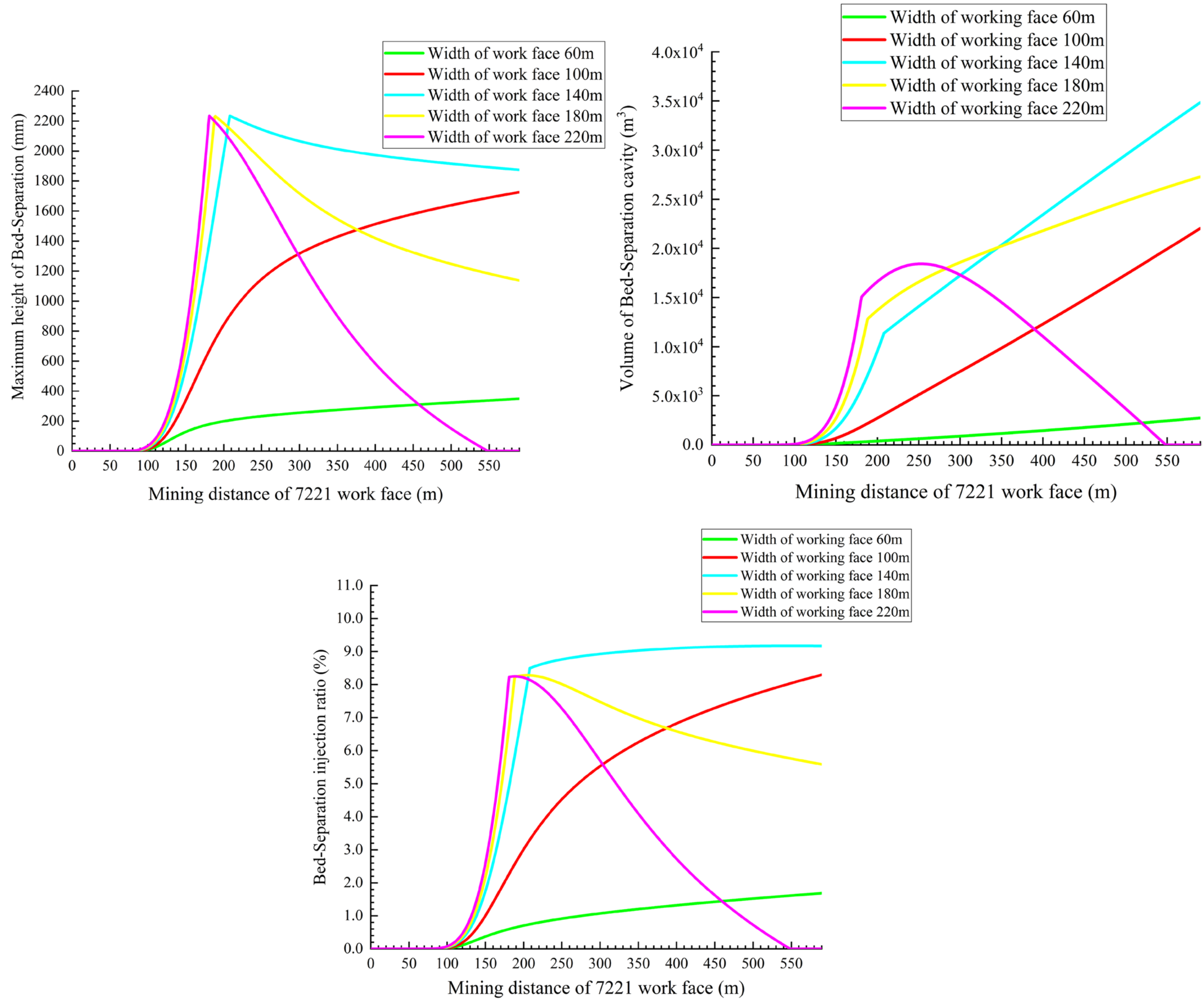

Fig. 11 Maximum height of Bed-separation development, Bed-separation volume, and non-pressure grouting injection ratio at different mining widths for hypothetical 7221 work face

the non-pressure slurry filling ratio, were measured for various mining widths in the 7221 work face, where Bed-separation slurry filling was employed. The findings are presented in Fig. 11. When the width of design mining reaches a point where it is considered sufficient for mining purposes, there is a noticeable increase in the height of Bed-separation development. Nevertheless, in the context of the mining operation where the working face is oriented in a forward direction, it is seen that the height of the Bed-separation development tends to diminish. Specifically, when the mining width measures 220 m, the Separation is entirely sealed off after a mining distance of 550 m. As the mining operation progresses to a distance of 588 m, it is observed that the volume of Bed-separation cavities in mining widths of 140 m and 180 m is greater compared to the mining width of 100 m.

Additionally, the non-pressure grouting injection ratio exceeds 6%. Nevertheless, the progress of separation exhibits more swiftness throughout its first stages. Consequently, when implementing Bed-separation slurry filling mining, it becomes imperative to elevate both the slurry injection rate and quantity. To design the suitable mining width for the 7221 work face, it is imperative to meticulously consider the integration of grouting holes and grouting equipment while also considering the input of grouting cost.

Table 6 presents comprehensive data on various aspects of the 7221 work face, including the precise locations of initial and final deflection, the maximum deflection values observed in the *PKS*, the volume of deflection space, the maximum height of bed-separation development, the volume of the bed-separation cavity, and the outcomes of non-pressure grouting injection ratios. These statistics are provided

Table 6 Results of *PKS* deflection and Bed-separation development assuming different mining widths for 7221 work face

Design width of work face (m)	*PKS* deflection start position (m)	*PKS* deflection end position (m)	*PKS* maximum deflection value (mm)	*PKS* deflection space volume (m^3)	Maximum height of Bed-separation (mm)	Maximum volume of Bed-separation cavity (m^3)	Maximum Bed-separation injection/production ratio (%)
Width of work face 60m	33	548	353.1	2768	347.8	2738	1.68
Width of work face 100m	30	548	1868	25,638	1725.2	22,053	8.29
Width of work face 140m	27	548	3999.6	65,098	2234.6	34,840	9.17
Width of work face 180m	24	548	3661.6	53,794	2232.1	27,242	8.28
Width of work face 220m	22	548	4903.9	72,087	2234.4	18,418	8.25

for different mining widths, offering a detailed analysis of the above-mentioned parameters. The visualization and comparative analysis of *PKS* deflection and Separation development may be achieved when considering the mining width of the proposed working face within the spectrum of adequate and inadequate mining conditions. Additionally, it confirms that the Isolated Overburden Grout Injection design necessitates that the mining width of the work face falls within the realm of insufficient mining.

Tendency non-sufficiently mining limit width parameter effects

After comparing the effects of different mining widths on the results of *PKS* deflection, Bed-separation height development, cavity volume, ground subsidence, and non-pressure grouting ratio, 7221 work face tended to realize full mining after reaching a mining width of 140 m. At this time, the indicators show a rapid increase, which poses a problem for mining ground subsidence control and grouting activities. While the actual design width of the 7221 work face is 100 m, to explore the detailed changes of each index of the limit mining width of the junction of non-full mining and full mining, at this point, it is still necessary to explore the changes of each index between the mining width of 100 m–140 m with a smaller mining width interval.

In this study, we have recalculated the *PKS* deflection, Bed-separation development height, Bed-separation cavity volume, and maximum ground subsidence values for a work face with mining widths of 110 m, 120 m, 130 m, and 140 m. The recalculated results are presented in Fig. 12. The figure illustrates the relationship between mining length, width, *PKS* deflection, and bed-separation development. When the mining length is 800 m and the mining width is 100 m, the *PKS* deflection and bed-separation development measure 1900 mm. Similarly, when the mining width is increased to 110 m, the *PKS* deflection and bed-separation development increase to 2800 mm, with the maximum height of bed-separation development reaching 2100 mm. Finally, when the mining width is further increased to 120 m, the *PKS* deflection and bed-separation development measure 3800 mm, with the bed-separation development height remaining 2100 mm. The bed-separation cavities exhibit a volume of approximately $4.2\times104m^3$ for widths ranging from 110 to 120 m, whereas a narrower width of 100 m results in a reduced volume of $3.4\times104m^3$. The observed ground subsidence values exhibited significant variation, with maximum measurements of 740 mm, 1077 mm, and 1369 mm corresponding to mining widths of 100 m, 110 m, and 120 m, respectively. The *PKS* deflection and bed-separation values significantly change when the mining width expands to 130 m and 140 m, respectively. These changes reach their peak value of 4000 mm when the mining length ranges from approximately 250 m to 400 m. Additionally, the maximum subsidence value of the ground exceeds 1000 mm, posing a substantial challenge for Bed-separation slurry filling mining. The height of the Bed-separation development and cavity volume do not exhibit substantial differences under mining widths of 130 m and 140 m compared to other design widths.

Mining height of the 7221 work face

The mining height of the 7221 work face refers to the thickness of the coal seam and gangue that is intended to be cut during the mining process. The mining height directly impacts the overall quantity of coal resources that can be removed, as well as the size of the mining extraction area. The closure of the Separation is achieved by progressively reconnecting the *PKS* flexure with the underlying strata as the mining operations proceed, facilitated by a limited mining height. The *PKS* deflection and bed-separation are only

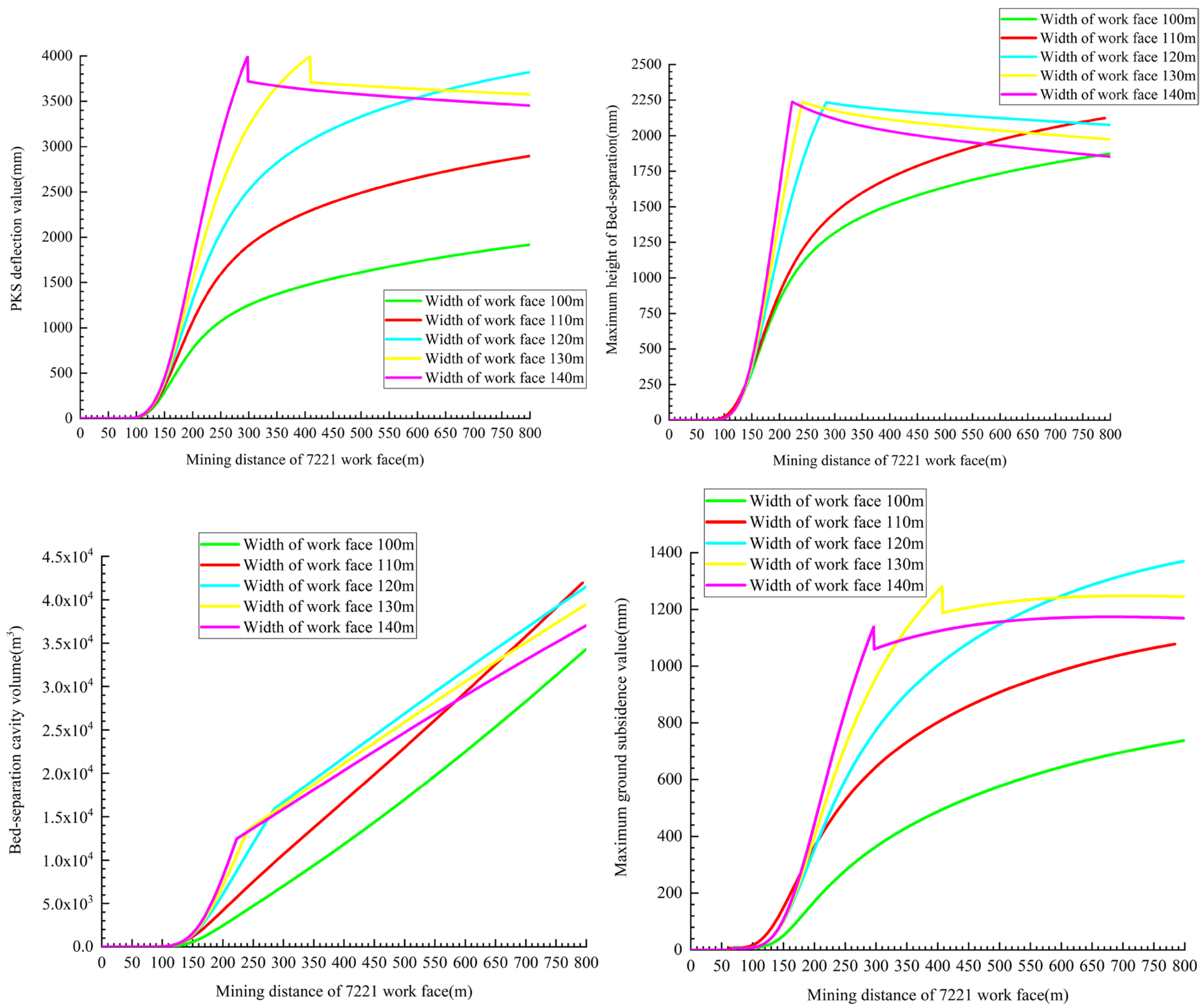

Fig. 12 Variation of *PKS* deflection and Bed-separation development height, Bed-separation cavity volume, and maximum ground subsidence value in 7221 work face with mining width 100 m-140 m

reconciled when the mining height reaches 1.6 m, and the mining distance exceeds 360 m. Consequently, the Bed-separation height experiences a quick reduction to zero. In all other mining height scenarios, bed-separation occurs beneath the *PKS*. The deflection of the *PKS* follows the same curve as a thin plate that is fully supported without any foundation support. Consequently, the deflection of the *PKS* at various mining heights is not currently subjected to detailed analysis.

Figure 13 displays the outcomes of determining the maximum height of Bed-separation development, the volume of Bed-separation cavities, and the non-pressure grouting injection ratio for the mining heights of 1.6 m, 2.6 m, 3.6 m, 4.6 m, and 5.6 m at the 7221 work face. Given that the underlying strata do not provide any support for *PKS* deflection and bed-separation beyond a mining height of 3.6 m, it can be observed that the maximum height of the off-separation development and the volume of the bed-separation cavity yield identical outcomes across all three scenarios, with the curves coinciding. As the 7221 work face progresses in mining, the mining height becomes smaller, increasing *PKS* deflection. Consequently, the *PKS* increasingly reconnects with the underlying strata, rapidly compressing the Bed-separation space. While the injection ratio of non-pressure grouting is larger in situations with less mining height, the closure

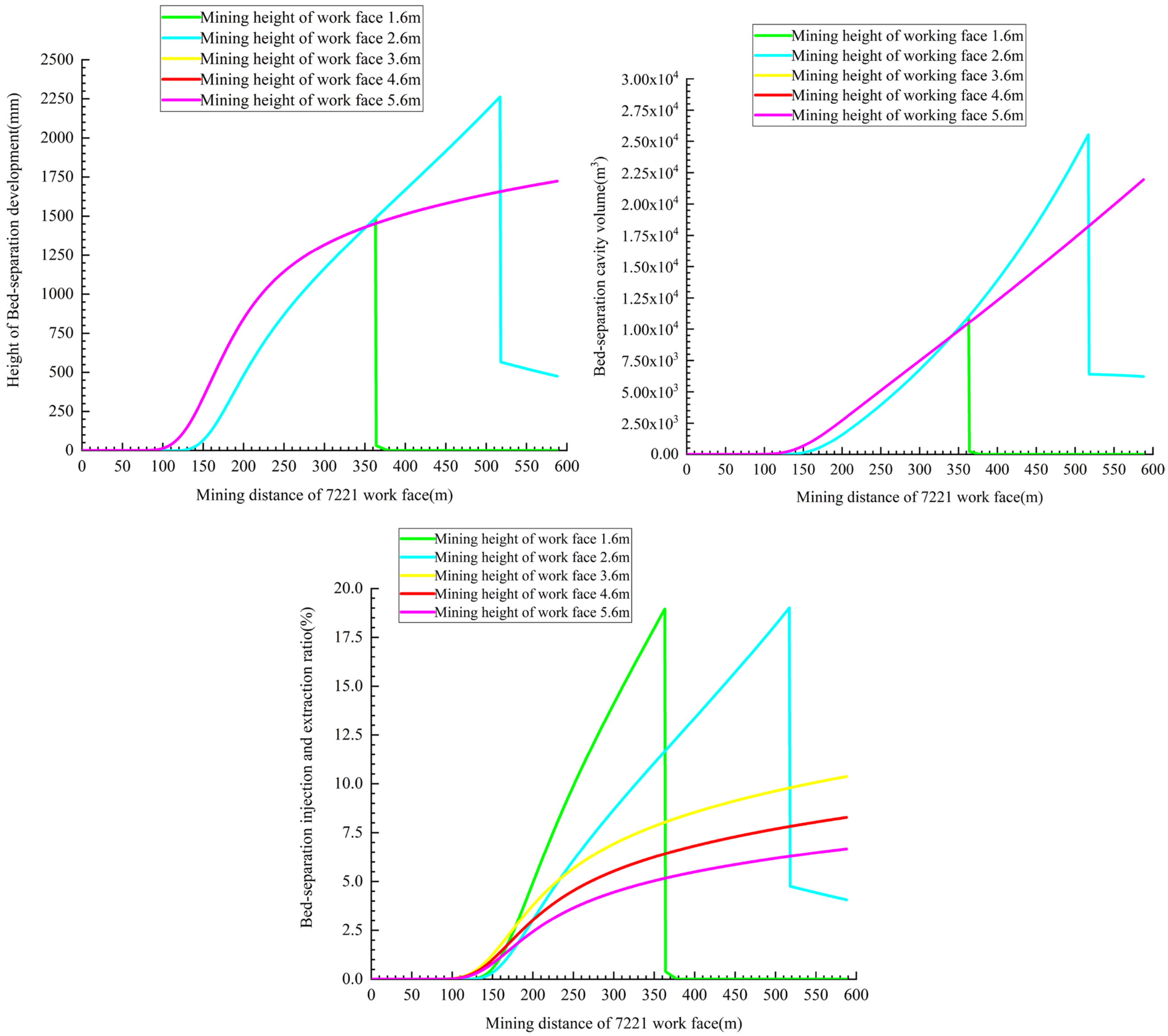

Fig. 13 Maximum height of Bed-separation development, volume of Bed-separation cavities, and non-pressure grouting injection ratio at different mining heights for hypothetical 7221 work face

of bed-separation occurs at a later stage, resulting in a smaller overall volume of the bed-separation cavity. The parameter design of the mining height of the working face is a critical factor in the extraction volume of coal resources and the economic returns when implementing Bed-separation slurry-filled mining.

Coal seam strike angle of 7221 work face

During the coal seam exploration process, determining the inclination angle between the strata and the coal seam is crucial. The working face strike angle can also be considered a stratigraphic parameter. Given that the model proposed in this study is a large-deflection inclined thin plate model, the authors aim to exploit the potential of the 7221 work face. It is assumed that the work face and the outer gangue are relatively thicker, allowing for mining at various strike angles throughout the operation. This paper examines the practical distinctions in the formation of *PKS* deflection and bed-separation resulting from the analysis of inclined coal seam mining under varying strike angles of the seam.

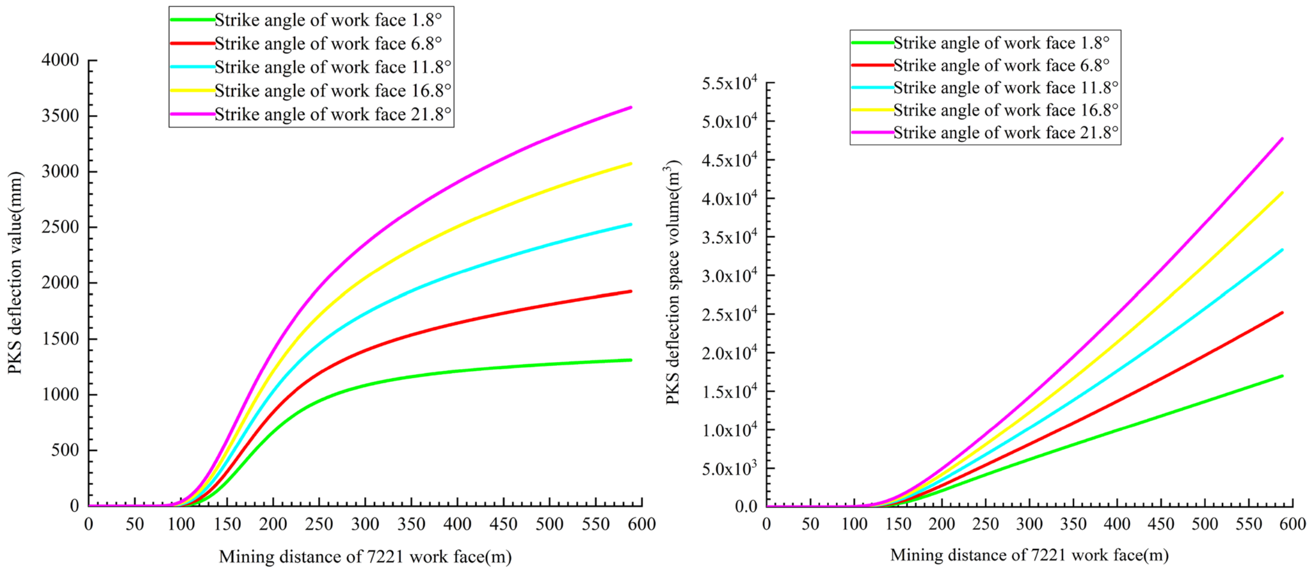

Fig. 14 Hypothetical *PKS* deflection values and volume of deflection space for different strike angles of the 7221 work face

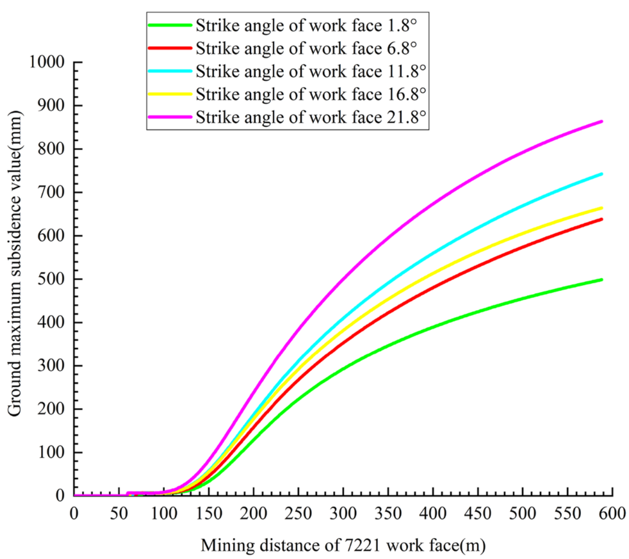

Fig. 15 Maximum subsidence values in the ground subsidence basin assuming different strike angles of the 7221 work face

7221 work face strike angle inclination effects on *PKS* deflection and ground subsidence

As the inclined seam is progressively mined, the depth of the working face mining line gradually rises, resulting in a linear increase in the overburden load above. The steady increase in the inclination angle of the coal seam leads to a corresponding increase in both the lateral load and mid-plane force, resulting in a gradual increase in the deflection value and deflection space volume of the *PKS*. Figure 14 illustrates the outcomes obtained from mining the 7221 work face at various strike angles, specifically to the *PKS* deflection values and the volume of deflection space. The fixed inclination angle of the coal seam is 8.2°. When the coal seam strike angle is 1.8°, it is commonly considered suitable for horizontal seam mining. When the coal seam strike angle is 21.8°, the deflection value of *PKS* is 3.5 times greater than that of horizontal seam mining, and the volume of the deflection space is estimated to be around three times larger. The inclination of the coal seam significantly influences the deflection of *PKS*. The conventional thin plate model exhibits several inaccuracies, which does not consider the coal seam inclination. These inaccuracies highlight the practical application value and significance of the large-deflection inclined thin plate model proposed by the authors of this research paper.

Calculations determined the impact of varying coal seam strike angles on the volume of *PKS* flexure space. Subsequently, the effect on the ground subsidence basin was assessed using the concept of isovolumetric behavior. The outcomes of this analysis are presented in Fig. 15. The maximum ground subsidence resulting from mining the coal seam with a strike angle of 21.8° is 1.6 times more than that of the coal seam with a strike angle of 1.8°, although it is still less than three times the value of the *PKS* flexural volume. The expansion of the ground-moving basin strike length occurs as the depth of coal seam mining grows. This phenomenon reduces the maximum ground sinking value while exerting a broader influence on the surrounding terrain.

The study involves the statistical mapping of several coal seams' strike inclination following the dynamic alteration of the maximum subsidence value of the ground throughout the progression of the working face. The characteristics measured in Table 7 include the length, width, basin volume, and

Table 7 Deformation results of ground subsidence basin with different strike angles for assuming 7221 work face

Strike angle of work face (°)	Length of subsidence basin (m)	Width of subsidence basin (m)	Ground maximum subsidence value (mm)	volume of subsidence basin (m^3)	Coordinates of center point of ground subsidence basin
Strike angle of 1.8°	765	340	499	20,067	(300.3,75)
Strike angle of 6.8°	795	346	640	30,300	(310.5,78)
Strike angle of 11.8°	821	352	742	39,375	(329.9,81)
Strike angle of 16.8°	857	356	664	48,140	(350.9,83)
Strike angle of 21.8°	901	362	863	56,407	(379.4,86)

coordinates of the subsidence basin's center point resulting from the coal seam's strike angles. The inclination of the working face strike has been observed to impact the length of the ground subsidence basin directly. Specifically, it has been noted that as the strike inclination of the working face increases, the length of the subsidence basin experiences

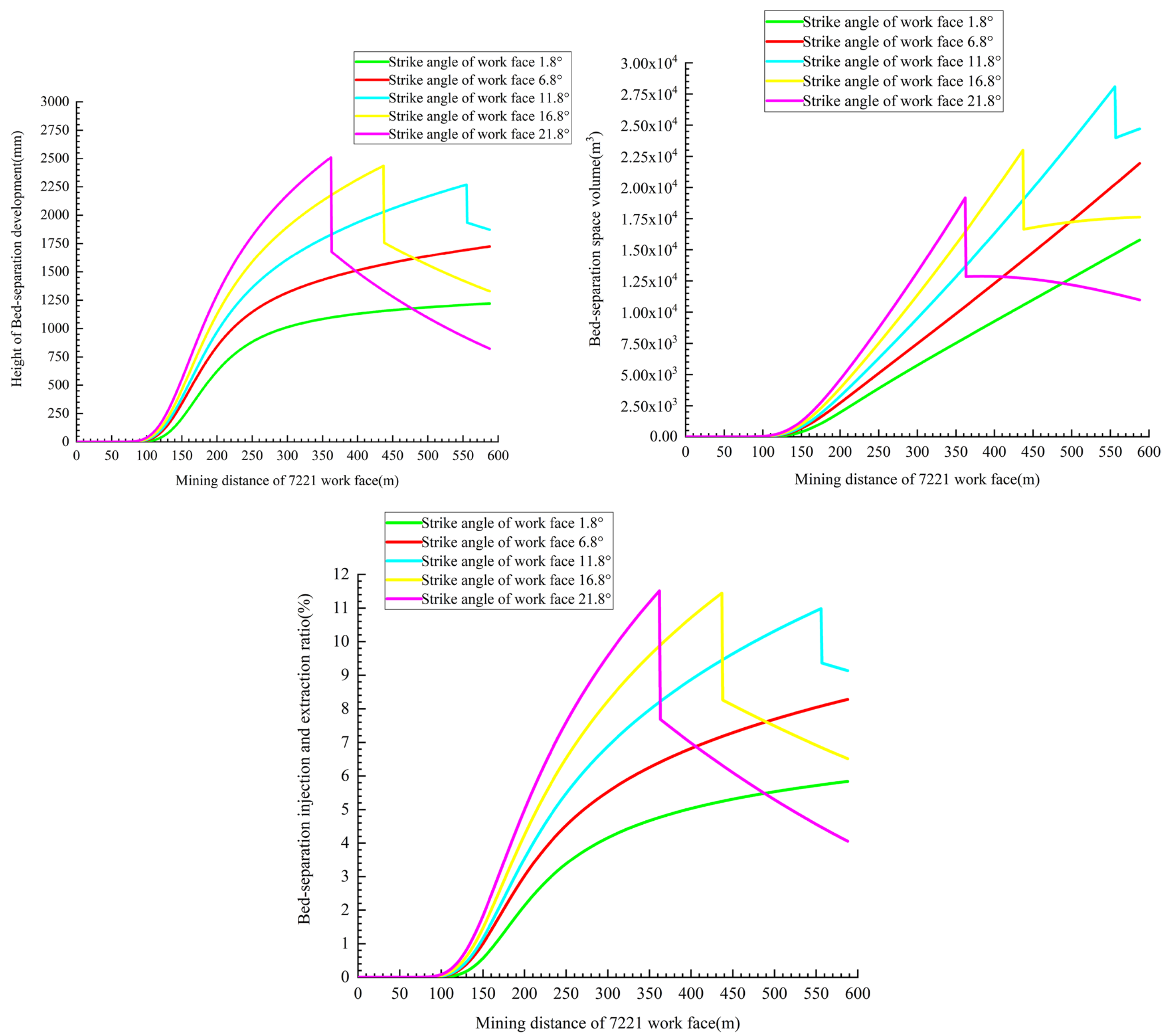

Fig. 16 Maximum height of Bed-separation development, Bed-separation volume, and non-pressure grouting injection ratio with different strike angles of 7221 work face

a significant increase beyond a mining distance of 588 m. This increase in length is accompanied by a simultaneous increase in both the maximum value of ground subsidence and the basin volume. The displacement of the central point of ground subsidence basins is influenced by the varying strike angles of coal seams, causing it to deviate from the center of the horizontal coal seams.

7221 work face strike angle impact on grouting design

The variation in the inclination of the coal seam results in a proportional rise in the lateral load and mid-plane force exerted on the *PKS* thin plate. Consequently, this leads to an escalation in the deflection of the *PKS* and the value of Bed-separation, thus impeding the progression of Bed-separation. The maximum height of the Bed-separation development, the volume of Bed-separation cavities, and the non-pressure grouting injection ratio were calculated using the large-deflection inclined thin plate model for various coal seams with different strike inclinations. The outcomes of these calculations are depicted in Fig. 16. As the inclination of the working face increases, there is a corresponding drop in the deflection value of the *PKS*, resulting in a reduction in both the height of the Bed-separation development and the volume of the Bed-separation cavities. When the mining distance is short, the slope of the coal seam strike leads to a greater development of Separation compared to the horizontal coal seam.

Given that the strike angle of a coal seam is a geological feature, it is imperative to thoroughly account for the impact of both the strike and inclination angles when determining the appropriate dimensions for the work face during design. Simultaneously, it is imperative to consider the impact of coal seam inclination when establishing the grouting holes. Consequently, it is recommended to position the grouting holes within the Bed-separation area beneath the *PKS*. The change in the inclination angle affects the stress release of the slurry, thereby altering the supporting action area of the *PKS*. This leads to deflection and bulge formation in the *PKS* thin plate. The precise outcomes of this phenomenon will be further elaborated upon in the subsequent section.

Table 8 provides a comprehensive statistical analysis of various parameters influenced by the strike inclination, including the start and end positions of *PKS* deflection, the maximum *PKS* deflection value and deflection space volume, the maximum height of Bed-separation development, the volume of Bed-separation cavities, and the non-pressure grouting injection ratio. The 7221 work face is assumed to be mined at a constant distance.

Design mining speed of 7221 work face

After the determination of the length, width, and height of the mining face in work 7221, it is observed that the mining rate does not have an impact on the final values of *PKS* deflection, deflection space volume, height of Bed-separation development, and Bed-separation cavity volume. Once the length has been established, the mining rate alone impacts the timing of these outcomes; specifically, the commencement of *PKS* deflection and Separation only occurs once they have reached their maximum values.

7221 work face mining speed effects on *PKS* deflection and ground subsidence

Figure 17 displays the results obtained from calculating the average mining speed of the 7221 work face based on its designated start and finish time. The mining speeds of 3 m/day, 5 m/day, 6 m/day, and 7 m/day were assumed, and the corresponding *PKS* deflection value and deflection space volume were calculated. The average mining speed of the 7221 work face was determined to be 4 m/day. The

Table 8 Hypothetical *PKS* deflection and Bed-separation development results for different strike angles of 7221 work face

Strike angle of work face (°)	*PKS* deflection start position (m)	*PKS* deflection end position (m)	*PKS* maximum deflection value (mm)	*PKS* deflection space volume (m^3)	Maximum height of Bed-separation (mm)	Maximum volume of Bed-separation cavity (m^3)	Maximum Bed-separation injection/production ratio (%)
Strike angle of 1.8°	29	542	1313	17,056	1220.9	15,861	5.84
Strike angle of 6.8°	30	548	1868	25,638	1725.2	22,053	8.29
Strike angle of 11.8°	31	553	2530	33,494	2268.6	28,006	10.97
Strike angle of 16.8°	31	557	3076	40,952	2434.3	23,005	11.44
Strike angle of 21.8°	31	560	3583	47,983	2509.9	19,167.4	11.51

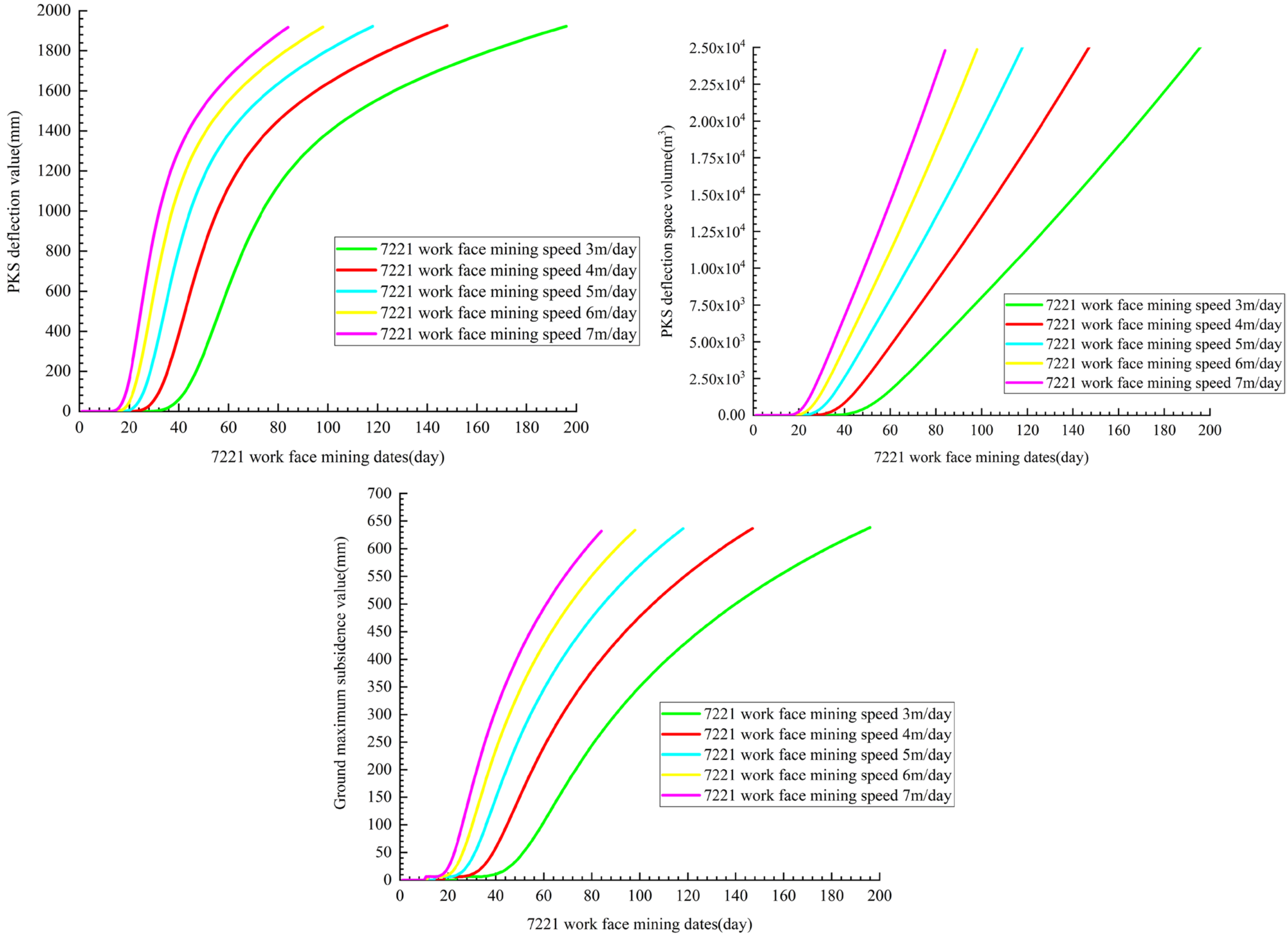

Fig. 17 Variation of *PKS* deflection value, deflection space volume, and ground subsidence with mining date for different mining speeds for assuming 7221 work face

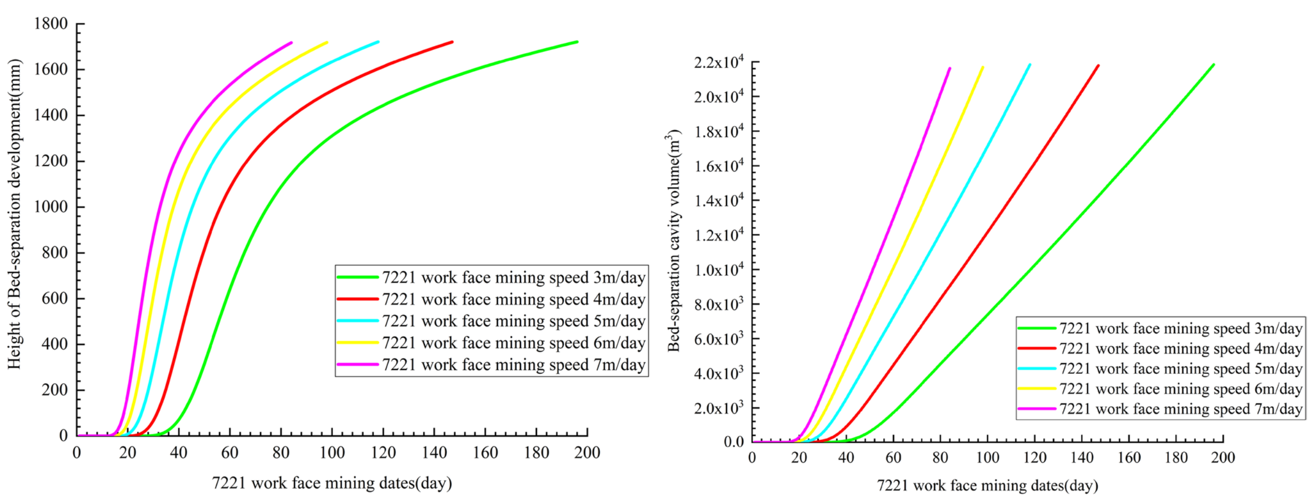

Fig. 18 Variation of Bed-separation development height and Bed-separation volume with mining time at different mining speeds for assuming 7221 work face

work face designated as 7221 has been specifically developed for mining operations spanning a distance of 588 m. A direct relationship exists between the speed of mining and the duration required to complete the mining process. Hence, the *PKS* deflection value and the volume of deflection space exhibit an earlier attainment of their maximum values, resulting in an escalation of the ground subsidence rate. The speed at which mining occurs directly impacts the speed at which Isolated Overburden Grout Injection must be performed. Failure to match the mining speed with the grouting speed can hinder the ability to manage the ground effectively.

7221 work face mining speed impact on grouting design

The variation in mining speeds for the 7221 work face does not impact the alteration of the maximum height of the Bed-separation development and the maximum value of the Bed-separation cavity volume. Nevertheless, its impact is confined solely to the rate at which the Bed-separation progresses. Figure 18 displays the outcomes of varying speeds in the design of the 7221 work face, resulting in dynamic changes in the development height of the Bed-separation and the volume of the Bed-separation cavity with the mining date. The rate at which mining occurs directly influences the pace of Bed-separation development and the duration of the reserved grouting interval. The mining speed's influence on the speed of Isolated Overburden Grout Injection (IOGI) grouting and the start and end time of grouting necessitates considering all three factors collectively for effective management of ground subsidence.

Effect of slurry filling parameters on *PKS* deflection and Bed-separation development and ground subsidence

The excavation of 7221 work face results in varying degrees of flexure and the creation of cavities in the above layers. The design parameters for the Isolated Overburden Grout Injection Technology included determining slurry injection holes, slurry injection start and stop time, and slurry concentration. The study employed a combination of the large-deflection inclined thin plate model and the slurry model to conduct a quantitative analysis of the impact of various grouting parameters on the deflection of *PKS* structures and ground subsidence. It is postulated that the quantity of slurry injected into the Bed-separation cavities did not surpass the capacity of the said cavities, neither in augmentation nor reduction. The completion date of slurry injection for all slurry holes, July 14, 2018, was not chosen. Instead, June 3, 2018, the completion date of mining at the 7221 work face, was selected for comparison.

Design number of grouting holes

When the grouting efficiency of each grouting hole is uniform, and the concentration of injected slurry remains constant, incorporating additional grouting holes will augment the grout injected concurrently. The grouting holes were positioned above the inclined centerline of the 7221 work face. Once the location of the first grouting hole was established, subsequent holes were placed consecutively at regular intervals of 50 m. The grouting holes were positioned along the centerline of the 7221 work face. In this study, the focus is on the design of slurry holes for mining purposes, specifically for the filling of work faces with slurry. The research assumes five slurry holes and aims to assess the impact of varying the number of slurry holes (specifically, 3, 4, 6, and 7) on the deflection value of *PKS*. The obtained results are presented in Fig. 19. The efficacy of *PKS* deflection control is compromised when the quantity of grouting holes is inadequate for properly managing *PKS* deflection. The attainment of the grouting threshold for Bed-separation cavities is expedited upon augmenting the quantity of grouting apertures. Furthermore, any elevation in grouting pressure or reduced efficacy will increase mining expenses. Hence, it is imperative to integrate the growth rate of Bed-separation cavities and the efficacy of grouting to determine an appropriate quantity of grouting orifices, ensuring optimal exploitation of each grouting orifice.

The completion date of mining at work, 7221, namely June 3, 2018, was determined. Additionally, calculations were conducted to assess the *PKS* lower *KS2* deflection, *PKS* deflection value, volume of deflection space, slurry injection volume, and maximum ground subsidence value. The lateral force of the formation and the downward squeezing impact of the slurry are subject to the deflection of *KS2*. This results in constructing a cavity with varying degrees of deflection when the grouting area intersects with *PKS*. The volume of deflection space in the *PKS* directly impacts the volume of the ground subsidence basin. The maximum value of ground subsidence can be estimated by identifying the dimensions and shape of the ground subsidence basin. Table 9 illustrates the impact of employing varying quantities of grouting holes on the deflection of *PKS* and the maximum values of ground sinking. The correlation between the number of injection holes and the volume of slurry injected into the Bed-separation cavity is positively associated with the effectiveness of *PKS* support. The decrease in *PKS* deflection value is accompanied by a reduction in the volume of the *PKS* deflection space, resulting in a decrease in the maximum

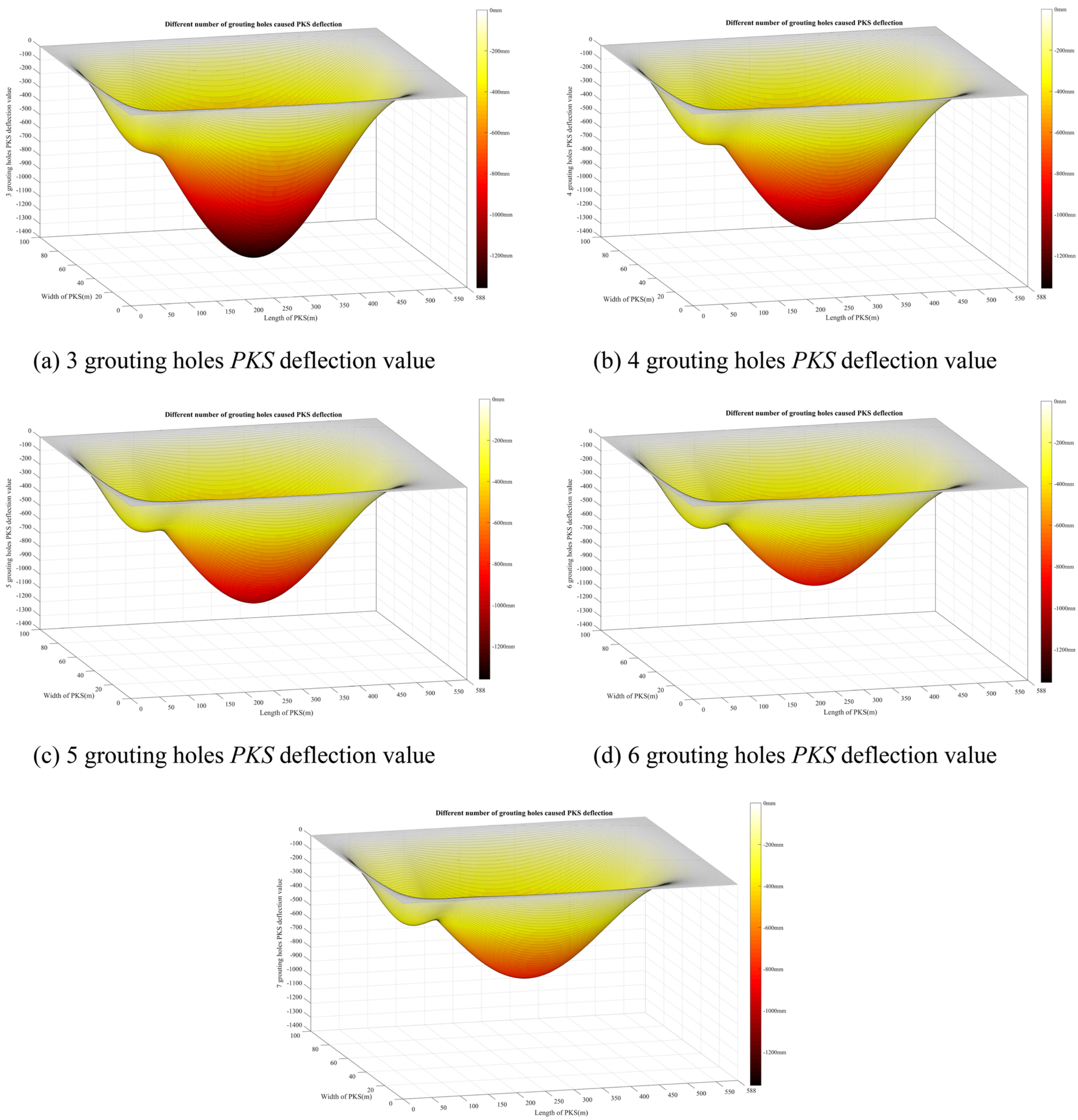

(a) 3 grouting holes *PKS* deflection value

(b) 4 grouting holes *PKS* deflection value

(c) 5 grouting holes *PKS* deflection value

(d) 6 grouting holes *PKS* deflection value

(e) 7 grouting holes *PKS* deflection value

Fig. 19 Effect of grouting with different number of grouting holes on *PKS* deflection value

value of ground sinking. This demonstrates effective control over ground subsidence.

Starting and stopping time of grouting

The implementation of slurry filling mining for the 7221 work face commenced on January 8, 2018, when the mining of the 7221 work face had reached a distance of 147 m. During a previous period, the mining distance of work face 7221 was observed to be relatively limited. Utilizing the large-deflection inclined thin plate model calculation; it was determined that deflection in the form of *PKS* commenced after the mining of the work face reached a distance of 71 m. Hence, the designated dates for grouting were established

Table 9 Effect of grouting with different number of grouting holes on *PKS* deflection and ground subsidence

Number of grouting holes	KS2 maximum deflection value (mm)	*PKS* maximum deflection value (mm)	*PKS* deflection space volume (m^3)	Slurry injection volume (m^3)	Ground maximum subsidence value (mm)
Three grouting holes	1993	1360	20,008	9285.6	– 498
Four grouting holes	2040	1160	17,078	12,380	– 428
Five grouting holes	2055	1020	15,253	15,476	– 354
Six grouting holes	2153	888	13,075	18,571	– 324
Seven grouting holes	2332	840	12,620	21,666	– 301

as January 29, 2018, February 13, 2018, March 3, 2018, and March 17, 2018, to align with the practical requirements of the mining operation. The 3D deflection function of *PKS* is determined by calculating the deflection at 7221 work face for various injection dates. The obtained findings are presented in Fig. 20. Due to the inclined nature of the seam mining in work face 7221, the slurry injection cannot adequately support the adjacent *PKS* along the open tangent line. Consequently, a bulge will form on the left side of the *PKS*. The smaller the volume of slurry injected into the Bed-separation cavity, the less effective it would be in providing support to the *PKS*, therefore necessitating a later start for the slurry injection. As of the commencement of slurry injection on March 17, 2018, it was observed that the slurry did not provide adequate support for the *PKS* until the completion of mining activities at the 7221 work face. The process of injecting grout into isolated overburden. Selecting an optimum date for slurry filling is crucial in properly managing ground sinking. Insufficient delay in the grouting process results in the inability of the Bed-separation cavity to retain the slurry, leading to the suspension of grouting instruments and subsequent escalation of grouting expenses. If the injection time is delayed, it is important to note that the ground may have already undergone significant sinking. Consequently, the injected slurry may not adequately mitigate the occurrence of ground subsidence.

Table 10 presents a comparative analysis of the impact of varying grouting start and finish times on *PKS* deflection and ground subsidence. The table includes calculations of KS2 and *PKS* deflection, together with corresponding values for the volume of space and maximum ground subsidence. According to the theoretical framework of the large-deflection inclined thin plate model, the calculation postulates that the Longwall mining operation conducted on the 7221 work face results in a maximum subsidence value of – 640 mm at ground level. Compared to the assumed initiation time of slurry, slurry filling mining plays a significant role in the management of ground subsidence. In pursuing efficient mining waste disposal and implementing environmentally friendly mining practices, the crucial factor in slurry design is carefully selecting optimal commencement and completion dates for grouting activities.

7221 work face Bed-separation grouting mining parameters optimization

The mining of work face 7221, the grouting of the Bed-separation cavity under *PKS*, and the control of ground subsidence are influenced by various parameters. These parameters can be categorized into three main aspects: stratigraphic parameters, design parameters of the work face, and parameters of the Bed-separation grouting slurry. The calculation of large-deflection inclined thin plates combined with the slurry model is used to analyze these parameters. The stratigraphic parameters encompass the *PKS* site's thickness, the main roof's thickness, and the lithology characteristics associated with stratigraphy. These parameters were established by the examination of the workings during the exploration process. The design parameters for the working face encompass various factors, such as the length and width of the working face, the mining height, the inclination of the coal seam, and the mining speed. The inclination of the coal seam is typically determined during the exploration phase of the working face. On the other hand, determining the mining height requires considering the impact of the coal mining machine and the roof support. It is important to note that these two parameters will remain unchanged in the context of this paper. The parameters for bed-separation grouting slurry encompass the quantity of grouting holes and the initiation and completion time of grouting. The design of slurry concentration should be based on the grouting pump power, the yield value of slurry in the grouting pipe, and parameters such as pressure drop and flow rate. It is important to note that the content of this paper will remain unaltered.

In brief, the optimization parameters on the 7221 work face for grouting encompass the length, width, and mining speed within the design limits of the work face. Additionally, the Bed-separation grouting slurry parameters encompass the number of grouting holes and the grouting start and end times. The primary aim of implementing slurry filling

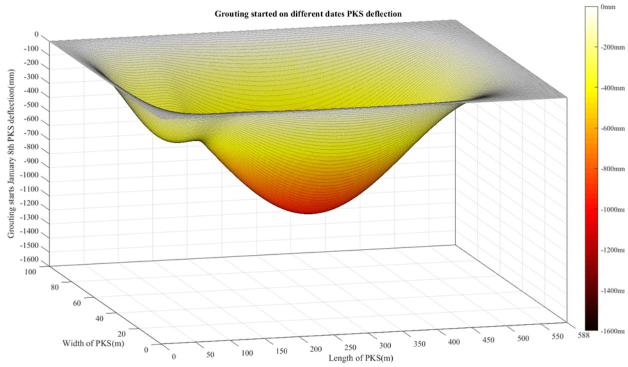

(a) Grouting holes started on January 8 *PKS* deflection values

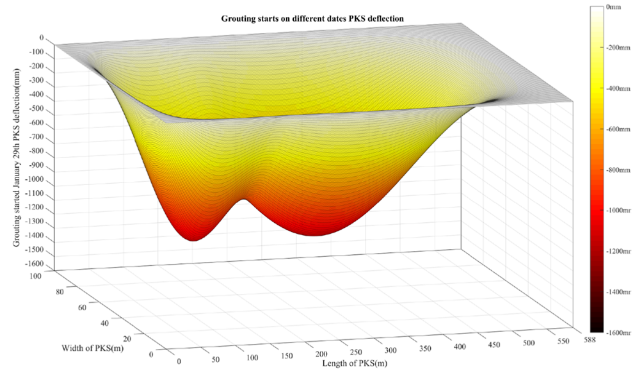

(b) Grouting holes started on January 29 *PKS* deflection values

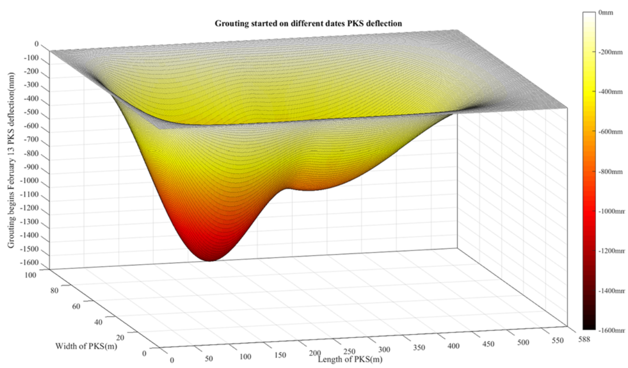

(c) Grouting holes started on February 13 *PKS* deflection values

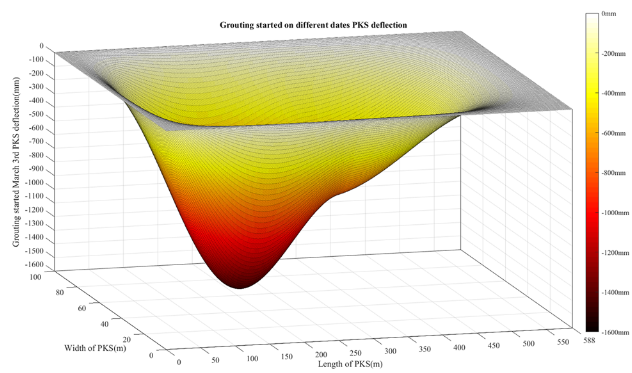

(d) Grouting holes started on March 3 *PKS* deflection values

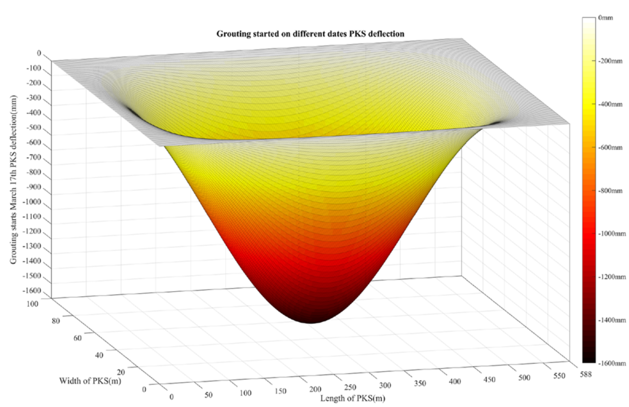

(e) Grouting holes started on March 17 *PKS* deflection values

Fig. 20 Effect of different grouting start and finish time selection on *PKS* 3D deflection

and mining activities at the 7221 work site is to manage ground subsidence effectively and ensure that the subsidence value within the protection zone of the neighboring villages remains below 10 mm. This objective is crucial due to the two villages close to the work as mentioned above face. Another objective of Isolated Overburden Grout Injection is to maximize the extraction of coal resources while simultaneously slurring the fly ash to facilitate trash filling and recycling, hence achieving environmentally sustainable mining practices.

Table 10 Effect of different grouting start and finish time selection on *PKS* deflection and maximum subsidence values

Grouting start date	Days to start mining (day)	KS2 maximum deflection value (mm)	*PKS* maximum deflection value (mm)	*PKS* deflection space volume (m^3)	Slurry injection volume (m^3)	Ground maximum subsidence value (mm)
January 8, 2018	33	2055	1020	15,253	15,476	– 354
January 29, 2018	54	2088	1148	16,862	13,826	– 438
February 13, 2018	69	2130	1288	18,965	12,340	– 486
March 3, 2018	86	2170	1465	21,380	10,523	– 553
March 17, 2018	100	2196	1552	22,800	9473	– 591

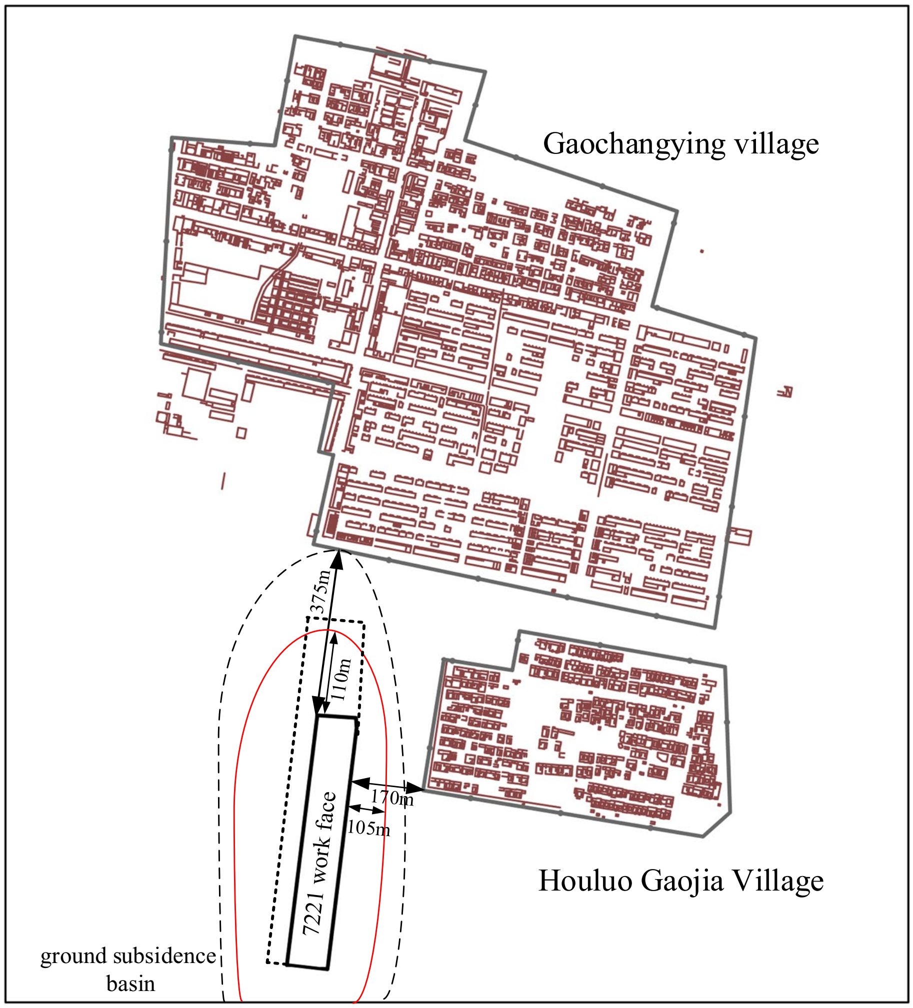

Fig. 21 Schematic of the optimization for 7221 work face mining ground subsidence basin expansion

Mining parameter optimization for 7221 work face

To ascertain the extension distance of the mining length and width of the work face, the spatial vertical distance between the 7221 work face and the two villages was re-measured. To maintain building subsidence values below – 10 mm in the two villages, it is necessary to accurately forecast the ground subsidence basin size. This will ensure that the village protection zones align with the tangent of the basin's inscribed function line. Figure 21 depicts the modified dimensions of the working face mining length and width and the associated ground subsidence basin. The current configuration of the 7221 work face entails a mining length of 588 m and a mining width of 100 m.

Additionally, the ground surface subsidence basin is characterized by a length of 794 m and a width of 376 m. A solid red line in the accompanying image visually represents the boundaries of this subsidence basin. To optimize the extraction of coal reserves and safeguard the integrity of the village structures, the operational front of the mining site was reconfigured, taking into account the dimensions of the subsidence basin, as indicated by the black dashed line in the diagram. According to the measurements, the distance between the work's opening cut line, face 7221, and Gaochangying village is 963 m. Additionally, it has been observed that the nearest point of the work face to the protection zone of Houlou Gaojia village is around 170 m.

Based on the observations depicted in Figs. 6, 7 and 8, it becomes evident that the complete extraction of the working face occurs when the mining width exceeds 140 m. Additionally, managing *PKS* deflection and Bed-separation filling mining, which is influenced by the *PKS* deflection and Bed-separation, becomes challenging when employing Bed-separation slurry filling mining. Consequently, limiting the work face mining width to less than 140 m is recommended to mitigate these difficulties. The objective is to modify the mining breadth of work face 7221 to increase its width downward while ensuring the subsidence basin engraved line does not encroach upon the protected area of Houlou Gaojia Village. The design of the ground subsidence basin includes an engraved line that extends tangentially along the strike expansion of the protection zone in Gaochangying village. This engraved line determines the mining length of the 7221 work face, which is designed to be 795 m. In Figs. 10, 11, the mining breadth of work face 7221 is observed to have been expanded by an additional 40 m. Consequently, the work face has reached its maximum mining capacity at a width of 140 m.

After determining the mining length of work face 7221, several mining widths were combined to design different mining speeds. This design considered the *PKS* deflection, Bed-separation development height, cavity volume, and maximum ground subsidence value. The initial operational face was engineered to achieve a mean excavation rate of

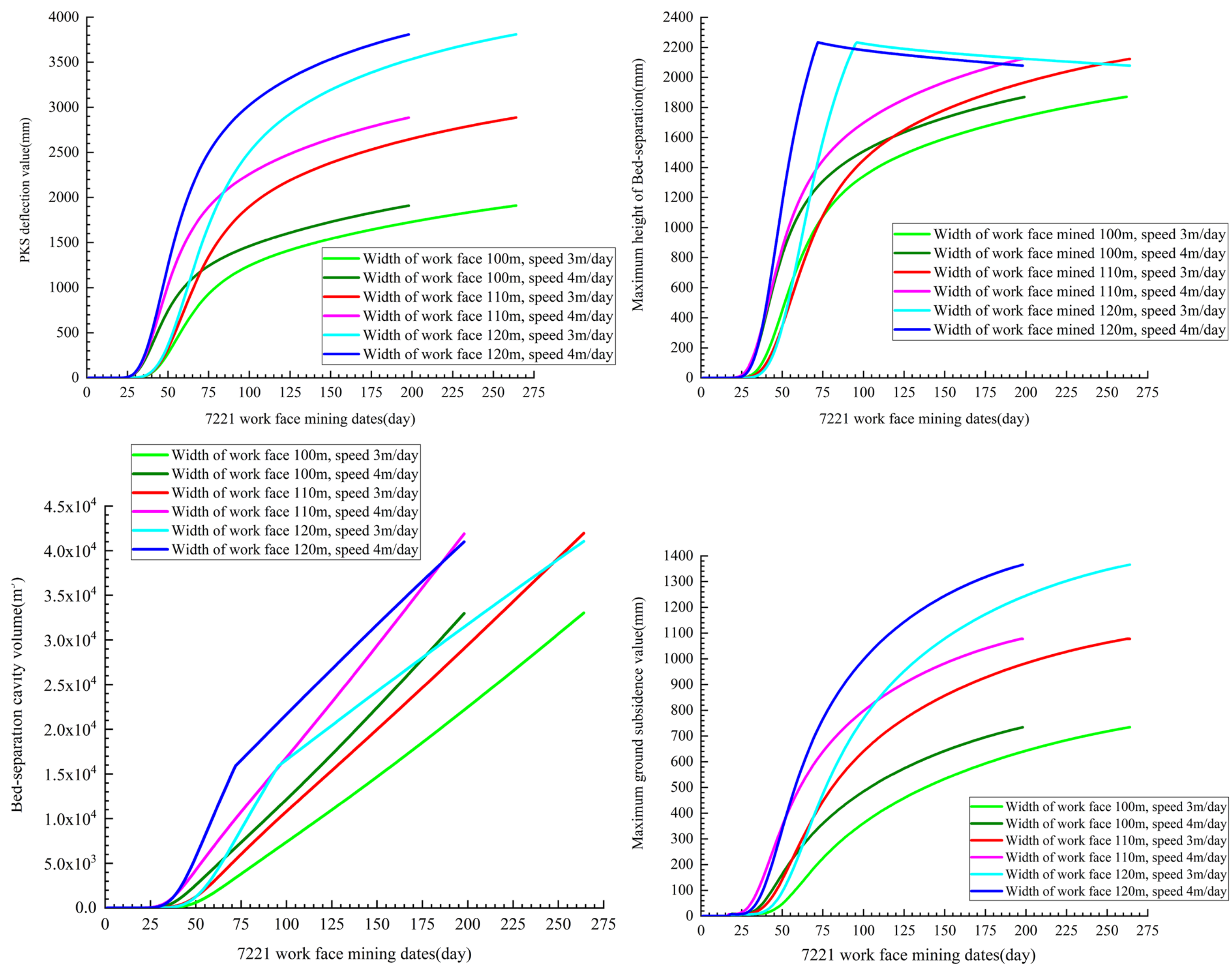

Fig. 22 Changes in *PKS* deflection value, height of Bed-separation development, Bed-separation cavity volume, and maximum ground subsidence value at different mining speeds for 7221 work face with mining width of 100 m-120 m

4 m per day, covering a total distance of 588 m over a mining duration of 147 days. Due to the expanded dimensions of mining in terms of length and width, the 7221 work face has been reconfigured to accommodate mining speeds of 3 m/day and 4 m/day. The outcomes of a comparative analysis, which involved assessing the deflection caused by mining-induced *PKS*, the development of bed-separation, and ground subsidence, are graphically presented in Fig. 22. The disparity in mining velocity solely impacts the mining process's temporal aspect and does not influence the ultimate outcomes. When comparing the rate of change for each deformation value, it is observed that for mining widths of 110 m and 120 m, the mining speed is 3 m/day. It is noted that the ultimate deformation value is bigger for these widths, but the pre-deformation speed is smaller compared to a mining width of 100 m, which has a speed of 4 m/day. Using specific mining parameters can effectively mitigate the challenges associated with controlling the *PKS* phenomenon and ground subsidence deformation during the initial stages of mining operations. By increasing the mining width and reducing the mining speed, it is possible to achieve the dual benefits of enhanced coal resource extraction and improved capacity for waste disposal through an increase in the volume of bed-separation cavities. Enlarging the mining breadth led to an augmentation in the magnitudes of the last deflection of the *PKS* and ground subsidence. Additionally, additional analysis and examination are required to thoroughly examine the outcomes of the final deformation after mining while using the bed-separation slurry filling technique.

Optimization of grouting parameters of the 7221 work face

Once the length, width, and mining speed dimensions for the 7221 work face have been established, the Isolated Overburden Grout Injection method is employed to define the parameters for slurry filling in the work face. This includes determining the number of slurry holes and the specific starting and finishing times for the slurry filling process. A linear relationship exists between the quantity of injection holes and the amount of slurry injected into the Bed-separation cavity. This relationship directly impacts the ultimate deflection of the *PKS* and the ground subsidence in the Bed-separation area. The initiation and termination of the grouting process are contingent upon the mining velocity. The grouting procedure will commence once the Bed-separation cavity has been sufficiently developed to satisfy the grouting criteria. Subsequently, the grouting holes will be terminated once the volume of the grouting slurry aligns with the predetermined design specifications.

The initial design of the mining length for the work face is 7221 m, with a width of 100 m. Additionally, there are a total of five grouting holes in the design. The current dimensions of the mining area are 795 m in length, with varying widths of 100 m, 110 m, and 120 m. The design of the volume of slurry injected into the Bed-separation cavity and the location of the slurry injection holes are based on the control requirements for ground subsidence and the volume of the Bed-separation cavity. The dimensions of the ground subsidence basin have been determined as follows: the length is 1059 m, and the width is 390 m. These measurements are based on the assumption that the maximum sinking value of the control ground is – 350 mm. Consequently, the predicted volume of the ground subsidence basin amounts to 22906m^3.

The isovolumetric concept determines that converting to the *PKS* flexural space volume amounts to 19,382m3. To meet the specifications for ground subsidence management, the grouting process must ensure a minimum volume of 19,382m3 for the Bed-separation cavity. The number of grouting holes can be determined by comparing the calculated volume of the Bed-separation cavity under various mining design parameters with the desired volume. Based on the grouting parameter statement, it was seen that the mean grouting volume for each grouting hole in the 7221 work face amounted to about 30m3/day. Furthermore, the grouting operation was successfully concluded 42 days after ceasing mining activities in the above-mentioned work. According to the parameter report, the commencement of the grouting

Table 12 Design of the number of grouting holes and grouting start and finish time with different mining parameters

Mining width, speed	Bed-separation cavity volume (m^3)	Number of grouting holes	Grouting start time	Grouting finish time	Grouting volume (m^3)	*PKS* deflection value (mm)
100m, 3m/day	33,989	7	January 25, 2018	August 29, 2018	47,793	976
100m, 4m/day	33,989	8	January 8, 2018	June 30, 2018	47,793	976
110m, 3m/day	41,946	11	January 20, 2018	August 28, 2018	79,553	892
110m, 4m/day	41,946	13	January 6, 2018	July 1, 2018	79,553	892
120m, 3m/day	41,273	13	January 17, 2018	August 31, 2018	97,608	816
120m, 4m/day	41,273	16	January 2, 2018	July 10, 2018	97,608	816

operation coincides with the arrival of the mining line at the initial grouting hole location.

Based on the theoretical framework of the large-deflection inclined thin plate combined with grouting model, it can be shown that when the pace of expansion of the Bed-separation cavity resulting from daily mining operations surpasses the rate of grouting, the slurry has a propensity to infiltrate the Bed-separation cavity readily. Consequently, this presents an opportune moment to initiate the grouting process. Regarding the growth rate of separation with varying widths and mining rates, as depicted in Fig. 17, it is observed that distinct mining velocities yield diverse initiation and completion periods for grouting. These outcomes are presented in Table 12. It is postulated that the initiation of mining at the 7221 work face coincided with the commencement of the original design on December 6, 2017. The completion of mining as per the original design occurred on June 3, 2018, while the grouting activities were concluded on July 14, 2018. The optimization of the 7221 work face will involve the integration of various mining parameters, such as the number of grouting holes, grouting start and finish time, and corresponding grouting volume. These parameters will be systematically organized in a table format to meet the requirements of ground subsidence control. Consequently, the deflection values of the *PKS* will also be recorded and are presented in Table 9.

Comprehensive Mining and Slurrying Parameters 7221 work face slurry filling mining plan selection

The implementation of Isolated Overburden Grout Injection was conducted in the 7221 work face to enhance the management of ground subsidence and safeguard the structural integrity of village structures. To maximize the acquisition of coal resources, the parameters for mining and grouting were optimized to align with the prevailing mining circumstances. To save the architectural structures of Gaochangying and Houlou Gaojia village, a comprehensive assessment of the 7221 work face's maximum mining length was conducted. The selection of the working face width was based on the requirement for the Bed-separation cavity volume to align with the fly ash waste handling capacity. Additionally, the deflection of *PKS* and the maximum deformation rate of Separation could be effectively managed by implementing grouting techniques. To ensure the timely and efficient execution of grouting activities, the design of various mining speeds is carefully coordinated to establish six distinct combinations of mining parameter design schemes. Upon consulting the initial design scheme, an estimation was made about the expected completion time for the grouting process. Additionally, the number of grouting holes and the designated start time for grouting were reconfigured by integrating the volume of the Bed-separation cavity and the typical rate of grouting per grouting hole.

Table 13 displays the mining and grouting parameter schemes that have been ultimately determined. A total of six schemes have been created. The variations in design widths result in differences in the *PKS* deflection value, deflection space volume, and Bed-separation cavity volume when the maximum subsidence of the control ground subsidence basin is – 350 mm. Consequently, the handling capacity of fly ash waste and mined coal resources also differs. Variations in mining speeds primarily dictate disparities in the durations of mining and grouting processes and the number of grout holes that need to be installed. When considering the protection requirements of ground buildings and the primary objectives of coal resource extraction and fly ash waste management, choosing a mining program with a bigger width among the options of 100 m, 110 m, and 120 m is advisable. The mining rate significantly impacts the duration of mining and grouting operations, and an extension of these activities results in higher mining and grouting expenses. The acceleration of mining operations leads to a quick increase in *PKS* deflection and ground subsidence values. To effectively regulate the thin plate, it is necessary to either increase the number of grouting holes and perform simultaneous grouting or enhance the power of the grouting pump. However, these measures also result in an escalated cost of grouting.

The initial dimensions of the work face 7221 are 588 m in length and 100 m in width. The average speed of progress

Table 13 Comparison of different mining and grouting scheme designs for 7221 work face with the original design

Mining width, speed	Percentage increase of coal resource extraction (%)	Duration of mining (day)	Duration of grouting (day)	Percentage increase of grouting volume (%)	Number of grouting holes
100m, 3m/day	135.2	265	216	308.8	7
100m, 4m/day	135.2	198	173	308.8	8
110m, 3m/day	148.7	265	220	514	11
110m, 4m/day	148.7	198	176	514	13
120m, 3m/day	162.2	265	226	630.7	13
120m, 4m/day	162.2	198	189	630.7	16

is 4 m per day. Additionally, there are a total of 5 grouting holes. These parameters may be found in Table 2 and Fig. 4. Table 12 compares the percentage increase in coal resource mining, mining, and grouting duration, volume of injected Bed-separation slurry, and the number of grouting holes for the original 7221 work face and the six mining design schemes mentioned above. Comparing the pros and disadvantages of each design scheme with the original design scheme can enhance the intuitive understanding, hence facilitating a more informed selection of the most suitable scheme for mining purposes.

Depending on the design alternatives for large-deflection inclined thin plate and grouting model, which consider various combinations of mining width and mining speed, each program exhibits distinct advantages and disadvantages. Consequently, a judicious selection should be made depending on the mining conditions. The completion of the 7221 work face in mining serves as the basis for the theoretical design presented in this study. The design is focused on comparing the effects of various mining and grouting parameters on the decision-making process of mining programs, considering the developed mechanical model. By formulating a more rational mining and grouting strategy, the objective is to achieve increased coal production while simultaneously implementing environmentally sustainable practices, minimizing the adverse effects on the surrounding ecosystem.

Conclusions

The paper utilizes the large-deflection inclined thin plate and slurry model to analyze the 7221 work face at the Huaibei mine. Following the modeling process to investigate the real subsidence and reduction effect of overburden isolation slurry filling mining technology, we proceed to analyze the impact of strata, mining, and slurry filling parameters on *PKS* deflection, Bed-separation development, and ground subsidence from a mechanical perspective. While maintaining all other parameters constant, the research parameters are regularly modified. The quantitative comparison of the influence of each parameter yields the following conclusions:

(1) The main roof's lithological characteristics directly impact the angle at which fractures occur in the main roof plate when subjected to pressure. The lithological factors significantly influence the deflection of *PKS*, the development of bed-separation, and the growth of the ground subsidence basin. It is important to meticulously extract and examine the lithological properties of these layers while developing the grouting strategy.

(2) The primary mining parameters under discussion encompass dimensions, such as length, width, and mining height, as well as factors like coal seam inclination and mining speed. These parameters are analyzed to determine their impact on *PKS* deflection, Bed-separation development, and ground subsidence. The coal bed inclination is a measurable metric used to detect the orientation of the working face. The dimensions of length, width, and height directly impact *PKS* deflection, bed-separation, and ground subsidence. The mining pace does not impact the outcome, but it does influence the timing and duration of bed-separation and the rate at which ground subsidence expands.

(3) The design parameters of slurry filling encompass the number of apertures and the initiation and cessation time. The number of grouting holes is proportional to the total amount and speed of grout injected into the Bed-separation cavity, assuming that each hole's grouting evaluation speed and volume are consistent. The initiation and cessation time of grouting is crucial for managing ground subsidence. The grouting time is now too premature. The formation of the bed-separation cavity is incomplete, resulting in delayed ground subsidence and a missed opportunity for optimal control.

(4) After analyzing the impact of stratigraphy, work face mining, and slurry design parameters, re-optimize specific mining and grouting parameters for the 7221 work face to improve performance. Efforts are made to mitigate ground subsidence in neighboring villages, raise the total quantity of coal resources extracted, and maximize the utilization of fly ash waste for backfilling.

Acknowledgements The authors are grateful to anonymous reviewers for their valuable suggestions.

Author contributions LI modeling article writing, MA provided study area and data, YANG provided financial support and writing guidance, JIANG gave advice on paper writing, GU, PENG, CHEN article review and submission work

Funding This research was supported by the Entrusted Project of Huaibei Mining Co., Ltd. (2023–129) and the National Natural Science Foundation of China [41971401].

Data availability The current study's data and source code can be found in this published article and its supplementary information file. The datasets generated and analyzed in the recent research and the source code are also available upon reasonable request to the corresponding authors.

Declarations

Conflict of interest The authors declare that they have no conflict of interest. The authors declare that they have no known competing financial interests or personal relationships that could have appeared to influence the work reported in this paper.

References

Alehossein H (2009) Viscous, cohesive, non-Newtonian, depositing, radial slurry flow. Int J Miner Process 93(1):11–19. https://doi.org/10.1016/j.minpro.2009.04.006. (**in English**)

Bo HZ et al (2023) Study on surface subsidence prediction method of shallow coal seam backfill-strip mining under the hard roof. Bull Eng Geol Environ 82(7):12. https://doi.org/10.1007/s10064-023-03284-3. (**Art no. 281, in English**)

Huang YC, Feng RM, Wang HP, Zhao WP, Liu YF (2011) the coal mining mode of paste-like fill and its application prospects. In: International Conference on civil engineering and building materials (CEBM), Kunming, PEOPLES R CHINA, Jul 29–31 2011, vol. 255–260, STAFA-ZURICH: Trans Tech Publications Ltd, in Advanced Materials Research, 2011, pp. 3744–3748, https://doi.org/10.4028/www.scientific.net/AMR.255-260.3744. [Online]. Available: <Go to ISI>://WOS:000302894902055

Jiang HQ, Fall M, Li YH, Han J (2019) An experimental study on compressive behaviour of cemented rockfill. Constr Build Mater 213:10–19. https://doi.org/10.1016/j.conbuildmat.2019.04.061. (**in English**)

Ju JF, Xu JL (2013) Structural characteristics of key strata and strata behaviour of a fully mechanized longwall face with 70 m height chocks. Int J Rock Mech Min Sci 58:46–54. https://doi.org/10.1016/j.ijrmms.2012.09.006. (**in English**)

Li WX, Gao CY, Yin X, Li JF, Qi DL, Ren JC (2015) A visco-elastic theoretical model for analysis of dynamic ground subsidence due to deep underground mining. Appl Math Model 39(18):5495–5506. https://doi.org/10.1016/j.apm.2015.01.003. (**in English**)

Li Z, Xu JL, Ju JF, Zhu WB, Xu JM (2018) The effects of the rotational speed of voussoir beam structures formed by key strata on the ground pressure of stopes. Int J Rock Mech Min Sci 108:67–79. https://doi.org/10.1016/j.ijrmms.2018.04.041. (**in English**)

Li Z, Feng GR, Cui JQ (2020) Research on the influence of slurry filling on the stability of floor coal pillars during mining above the room-and-pillar goaf: a case study. Geofluids. https://doi.org/10.1155/2020/8861348. (**Art no. 8861348, in English**)

Li J, Xuan DY, Xu JL, Dong ZB, Wang CC (2023) Compaction response of mining-induced rock masses to longwall overburden isolated grouting. Minerals 13(5):15. https://doi.org/10.3390/min13050633. (**Art no. 633, in English**)

Liu Y, Guo WJ, Chen JT (2012) Study on the technique of filling paste into mine goaf with building waste. In: 2nd International Conference on Applied Mechanics, Materials and Manufacturing (ICAMMM 2012), Changsha, PEOPLES R CHINA, Nov 17–18 2012, vol. 268–270, STAFA-ZURICH: Trans Tech Publications Ltd, in Applied Mechanics and Materials, 2013, pp 656–659, doi: https://doi.org/10.4028/www.scientific.net/AMM.268-270.656. [Online]. Available: <Go to ISI>://WOS:000320476800136

Palarski J (1989). The experimental and practical results of applying backfill. In: Hassani FP, Scoble MJ, Yu TR (eds) Innovations in mining backfill technology—Proceeding of the 4th International Symposium on Mining with Backfill. Rotterdam: Balkema, 1989, pp 33–37

Qian M, Xu J, Miao X (2003) Green technique in coal mining. J China Univ Min Technol 32(4):343–348

Tan YL, Liu XS, Ning JG, Tian CL (2015) Front abutment pressure concentration forecast by monitoring cable-forces in the roof. Int J Rock Mech Min Sci 77:202–207. https://doi.org/10.1016/j.ijrmms.2015.04.002. (**in English**)

Wang YX et al (2022) "Reform and development of coal mine safety in China: an analysis from government supervision, technical equipment, and miner education. Resour Policy 77:14. https://doi.org/10.1016/j.resourpol.2022.102777. (**Art no. 102777, in English**)

Wang BL, Xu JL, Xuan DY (2018) Time function model of dynamic surface subsidence assessment of grout-injected overburden of a coal mine. Int J Rock Mech Min Sci 104:1–8. https://doi.org/10.1016/j.ijrmms.2018.01.044. (**in English**)

Xu J, Xuan D, Zhu W (2015) Study and application of coal mining with partial backfilling. J China Coal Soc 40(6):1303–1312

Xuan DY, Xu JL (2017) Longwall surface subsidence control by technology of isolated overburden grout injection. Int J Min Sci Technol 27(5):813–818. https://doi.org/10.1016/j.ijmst.2017.07.014. (**in English**)

Xuan DY, Xu JL, Wang BL, Teng H (2015) Borehole investigation of the effectiveness of grout injection technology on coal mine subsidence control. Rock Mech Rock Eng 48(6):2435–2445. https://doi.org/10.1007/s00603-015-0710-5. (**in English**)

Xuan DY, Xu JL, Wang BL, Teng H (2016) Investigation of fill distribution in post-injected longwall overburden with implications for grout take estimation. Eng Geol 206:71–82. https://doi.org/10.1016/j.enggeo.2016.04.007. (**in English**)

Xuan DY, Li J, Zheng KD, Xu JL (2020) Experimental study of slurry flow in mining-induced fractures during longwall overburden grout injection. Geofluids. https://doi.org/10.1155/2020/8877616. (**Art no. 8877616, in English**)

Yang SM, Zhang GR (2012), Study on technologies and countermeasures of comprehensive utilization of coal resources. In: International Conference on sustainable energy and environmental engineering (ICSEEE 2012), Guangzhou, PEOPLES R CHINA, Dec 29–30 2012, vol. 295–298, STAFA-ZURICH: Trans Tech Publications Ltd, in Applied Mechanics and Materials, 2013, pp. 3001–3004, doi: https://doi.org/10.4028/www.scientific.net/AMM.295-298.3001. [Online]. Available: <Go to ISI>://WOS:000320828201247

Yin W, Wang JQ, Bai XM, Sun WJ, Zhou ZY (2020) Strata behavior and control strategy of backfilling collaborate with caving fully-mechanized mining. Open Geosci. 12(1):703–717. https://doi.org/10.1515/geo-2020-0168. (**in English**)

Zhao DS, Xu T, Tang CA, Fan XL (2001) Numerical simulation of bed separation of overburden strata induced by mining excavation. In: ISRM International Symposium/3rd Asian Rock Mechanics Symposium (ARMS), Kyoto, JAPAN, Nov 30-Dec 02 2004, ROTTERDAM: Millpress Science Publishers, 2004, pp 475–478. [Online]. Available: <Go to ISI>://WOS:000228664700075. [Online]. Available: <Go to ISI>://WOS:000228664700075

Zhu JM, Ma ZW, Xu JH, Wu JN (2011) Research on the technology of filling and repeated mining in thick coal seam affected by small mine gob area. In: 1st International Symposium on Mine Safety Science and Engineering (ISMSSE), Beijing, PEOPLES R CHINA, Oct 26–29 2011, vol. 26, AMSTERDAM: Elsevier Science Bv, in Procedia Engineering, 2011, https://doi.org/10.1016/j.proeng.2011.11.2285. [Online]. Available: <Go to ISI>://WOS:000300848300153

Zhu WB, Xu JM, Xu JL, Chen DY, Shi JX (2017) Pier-column backfill mining technology for controlling surface subsidence. Int J Rock Mech Min Sci 96:58–65. https://doi.org/10.1016/j.ijrmms.2017.04.014. (**in English**)